Hotei M, Billal DS, Togawa A, Ikeda Y, Takei S, Kono M, Ogami M, Ubukata K, Sugita R, Fujihara K, Yamanaka N.	Distribution of fibronectin-binding protein genes (prtF1 and prtF2) and streptococcal pyrogenic exotoxin genes (spe) among Streptococcus pyogenes in Japan.	J Infect Chemother	15	367-373	2009
Oma K, Zhao J, Ezoe H, Akeda Y, Koyama S, Ishii KJ, Kataoka K, Oishi K.	Intranasal immunization with a mixture of PspA and a Toll-Like Receptor Agonist induces specific antibodies and enhances bacterial clearance in the airways of mice.	Vaccine	27	3181-3188	2009
Hasegawa H, Ichinohe T, Ainai A, Tamura S, Kurata T.	Development of mucosal adjuvants intranasal vaccine for H5N1 influenza virus.	Ther Clin Risk Manag	Feb;5(1)	125-32	2009
Nakamura A, Sakano T, Nakayama T, Shimoda H, Okada Y, Hanayama R, Nomoto K, Suto T, Kinoshita Y, Furue T, Ono H, Ohta T.	Neonatal pertussis presenting as acute bronchiolitis: direct detection of the Bordetella pertussis genome using loop-mediated isothermal amplification.	Europ J Ped	168(3)	347-349	2009
Fukasawa C, Ishiwada N, Ogita J, Hishiki H, Kohno Y.	The effects of disodium cromoglycate on enhanced adherence of *Haemophilus influenzae* to A549 cells infected with respiratory syncytial virus.	Pediatr Res	66	168-73	2009

IV　研究成果の刊行物・別刷

ORIGINAL RESEARCH

Differences of Clinical Manifestations According to the Patterns of Brain Lesions in Acute Encephalopathy with Reduced Diffusion in the Bilateral Hemispheres

A. Okumura
H. Kidokoro
T. Tsuji
M. Suzuki
T. Kubota
T. Kato
M. Komatsu
T. Shono
F. Hayakawa
T. Shimizu
T. Morishima

BACKGROUND AND PURPOSE: The precise clinical characteristics of acute encephalopathy with bilateral reduced diffusion are not fully understood. We compared clinical, laboratory, and neuroimaging findings according to the patterns of brain lesions among children with reduced diffusion in the bilateral hemispheres.

MATERIALS AND METHODS: Nine patients were analyzed. The patterns of brain lesions were divided into diffuse lesions and central-sparing lesions. Diffuse lesions were defined as reduced diffusion in the whole cortex and/or subcortical white matter. Central-sparing lesions were defined as the lack of reduced diffusion in the areas around the bilateral Sylvian fissures. Clinical, laboratory, and neuroimaging findings were compared between groups.

RESULTS: Five patients showed diffuse lesions and 4 showed central-sparing lesions. Coma was significantly more common in patients with diffuse lesions, whereas a biphasic clinical course was more common in those with central-sparing lesions. Outcome was worse in patients with diffuse lesions. Maximal aspartate aminotransferase, alanine aminotransferase, and kinase levels were also significantly higher in patients with diffuse lesions. In 2 patients with diffuse lesions, diffusion-weighted images during the acute phase revealed reduced diffusion in the bilateral frontal and occipital areas, followed by diffuse lesions. No patient with central-sparing lesions showed MR imaging abnormalities during the acute phase.

CONCLUSIONS: Clinical manifestations in patients with diffuse lesions were severe, whereas those in patients with central-sparing lesions were relatively mild.

Acute encephalopathy in association with infectious disease has attracted the attention of pediatricians and pediatric neurologists in Japan since the outbreak of influenza-associated encephalopathy during the 1997/1998 winter season. Every year, it is estimated that hundreds of Japanese children die or experience neurologic sequelae due to acute encephalopathy of infectious causes, which has prompted studies on acute encephalopathy in Japan. Recent studies have revealed several patterns of neuroimaging abnormalities in children with acute encephalopathy. Acute necrotizing encephalopathy is characterized by the presence of multiple symmetric brain lesions in the bilateral thalami and other specific brain regions, such as the periventricular white matter and internal capsule.[1] Clinically mild encephalitis/encephalopathy with a reversible splenial lesion is characterized by transient reduced diffusion in the splenium of the corpus callosum, with complete recovery.[2]

Recently, Takanashi et al[3] described a form of acute encephalopathy characterized by biphasic seizures and late reduced diffusion (AESD). In patients with AESD, a seizure, especially a prolonged one, is commonly observed at onset. The following day, patients appear relatively well and seem to have recovered consciousness almost fully, though slightly reduced responsiveness, an absent-minded appearance, or subtle disorientation may be apparent. Deterioration of consciousness, clustered seizures, and involuntary movements appear 3–7 days after the first seizure. Furthermore, this subtype of acute encephalopathy is characterized by widespread reduced diffusion on MR imaging from 3 to 9 days after onset. Although the outcome of patients with AESD is reportedly very poor,[3] a milder form of AESD without neurologic sequelae has also been described.[4] It is interesting that all reported cases of children with AESD have been of in those of East Asian descent.[5]

At present, the precise clinical characteristics of AESD are not fully understood. For example, it is uncertain whether a biphasic clinical course is always observed in children with AESD. It is also unclear whether reduced diffusion is always absent on MR imaging within 2–3 days after onset. We compared the clinical manifestations, laboratory data, and MR imaging features of children with reduced diffusion in the bilateral hemispheres, according to the patterns of brain lesions, to better understand the spectrum of this subtype of acute encephalopathy associated with infection.

Received August 29, 2008; accepted after revision October 26.

From the Department of Pediatrics (A.O., T. Shimizu), Juntendo University School of Medicine, Tokyo, Japan; Department of Pediatrics (A.O., T. Shono, M.K.), Urayasu Ichikawa Municipal Hospital, Chiba, Japan; Department of Pediatrics (H.K., T. Kubota), Anjo Kosei Hospital, Anjo, Japan; Department of Pediatrics (T.T., M.S., T. Kato, F.H.), Okazaki City Hospital, Okazaki Japan; and Department of Pediatrics (T.M.), Okayama University Graduate School of Medicine and Dentistry, Okayama, Japan.

The data in this manuscript were collected from many hospitals. The first 9 authors were attending pediatric neurologists and contributed to the collection of clinical data. Dr Toshiaki Shimizu helped to integrate the clinical data. Dr Tsuneo Morishima supervised this study. These 2 coauthors also contributed to the writing of this manuscript.

This work was supported by the grant from the Japanese Ministry of Education, Culture, Sports, Science and Technology (20249053).

Please address correspondence to Akihisa Okumura, MD, Department of Pediatrics, Juntendo University, School of Medicine, 2-1-1 Hongo, Bunkyo-ku, Tokyo, 113-8421, Japan; e-mail: okumura@juntendo.ac.jp

DOI 10.3174/ajnr.A1431

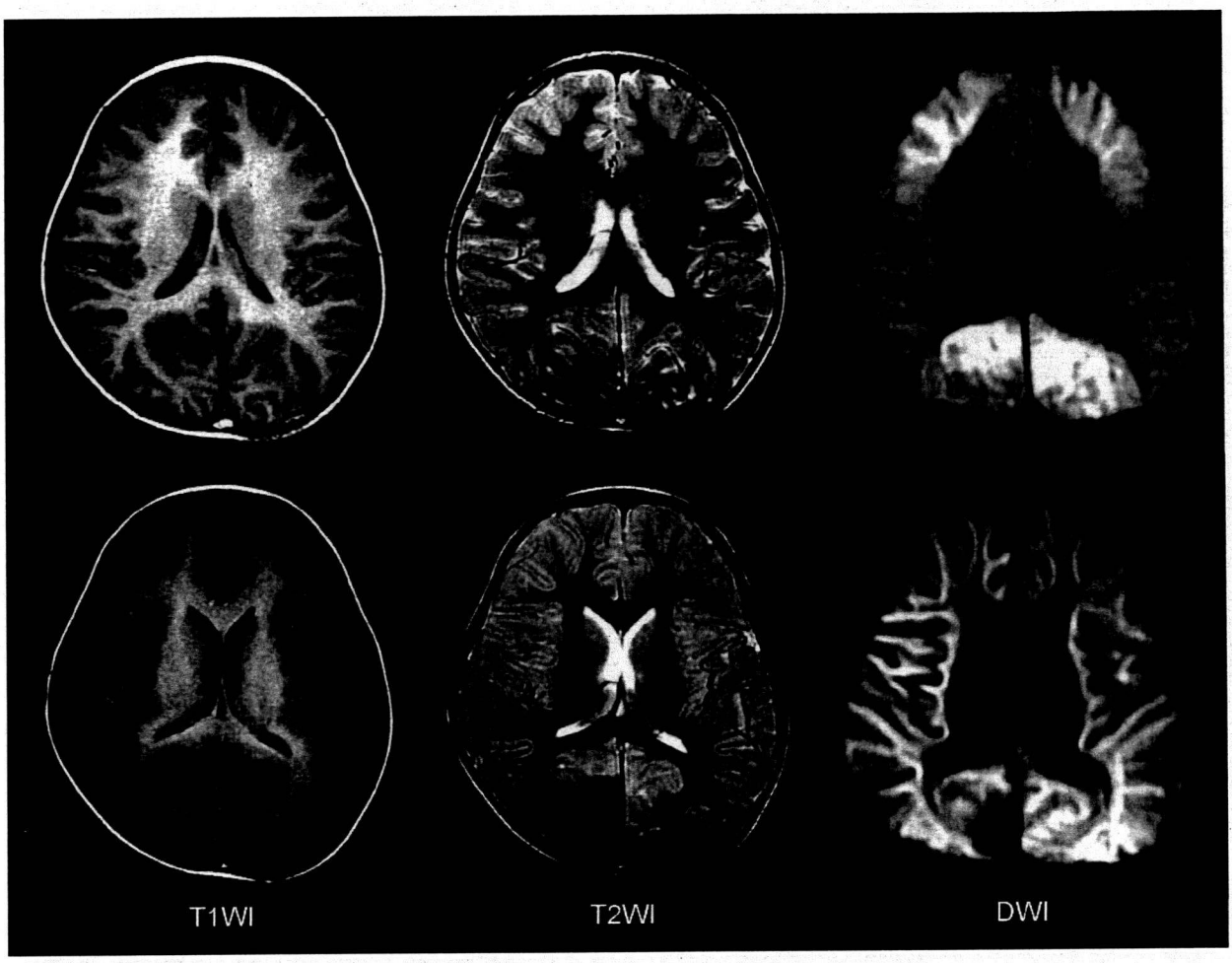

Fig 1. MR imaging findings of a patient with diffuse lesions. Top: The day after the onset, T1-weighted (T1WI) images show mild thickening of the cortex and T2-weighted (T2WI) images reveal mildly increased intensities in the cortex of the bilateral frontal lobes. Reduced diffusivity is observed in the bilateral frontal and occipital regions on DWIs (frontal occipital lesions). Bottom: Five days after the onset, T1WI and T2WI images demonstrate marked edematous changes in the entire cortex. Reduced diffusivity is observed in the entire subcortical white matter on DWIs.

Materials and Methods

We identified 79 children (age, ≤15 years) with acute encephalopathy who were admitted to the Department of Pediatrics at Nagoya University Hospital, Juntendo University Hospital, and 13 affiliated hospitals between January 2000 and August 2007. Acute encephalopathy was defined as a condition characterized by decreased consciousness with or without other neurologic symptoms, lasting for >24 hours in children with infectious symptoms, such as fever, cough, and diarrhea. We carefully excluded patients with sustained decreased consciousness after a febrile seizure, and those with delirious behavior without obviously reduced consciousness. We also excluded patients who were clinically diagnosed with status epilepticus by the attending physician. In this study, a prolonged seizure was defined as one lasting for >20 minutes. Coma was defined as a condition in which the patient was not arousable with maximal painful stimulation, which is consistent with a score of 3–5 on the Glasgow Coma Scale, modified for children, or a score of 100–300 on the Japan Coma Scale.

MR imaging was performed in 65 of 79 patients, and diffusion-weighted images (DWIs) were obtained in 37 patients. Among these, 9 patients showed widespread reduced diffusion in the cortex and/or subcortical white matter of the bilateral hemispheres. These 9 patients became the subjects of this study. In these patients, DWIs were generated by using a 1.5T unit, with a spin-echo echo-planar imaging sequence with variable settings (TE, 86–109 ms; TR, 3066–4100 ms; 952- to 1445-Hz/pixel bandwidth; echo-planar factor, 53–128; section thickness, 5.0–6.0 mm). MR spectroscopy was not performed in any patient.

Two distinct patterns of brain lesions were recognized in DWI: diffuse lesions and central-sparing lesions (Figs 1 and 2). Diffuse lesions were defined as reduced diffusion in the whole cortex and/or subcortical white matter in the bilateral hemisphere during the clinical course. In some patients, reduced diffusion in the frontal and occipital areas preceded diffuse lesions. Central-sparing lesions were defined as the lack of reduced diffusion in the areas around the bilateral Sylvian fissures, though diffuse abnormalities were typically present in other areas on MR imaging. All MR imaging data were reviewed by the chief author (A.O.), with the attending physicians.

Laboratory data were also assessed from medical records. We investigated the following values: platelet counts; aspartate aminotransferase (AST), alanine aminotransferase (ALT), lactate dehydrogenase, creatinine kinase, blood urea nitrogen, creatinine, glucose, and ammonia levels; and cell counts and protein in the CSF. Some of these values were evaluated in previous studies as prognostic factors of acute encephalopathy.[6,7] Nagao et al[6] revealed that elevated AST levels, hyperglycemia, the presence of hematuria or proteinuria, and the use of diclofenac sodium were associated with poor outcomes in children with influenza-associated encephalopathy.

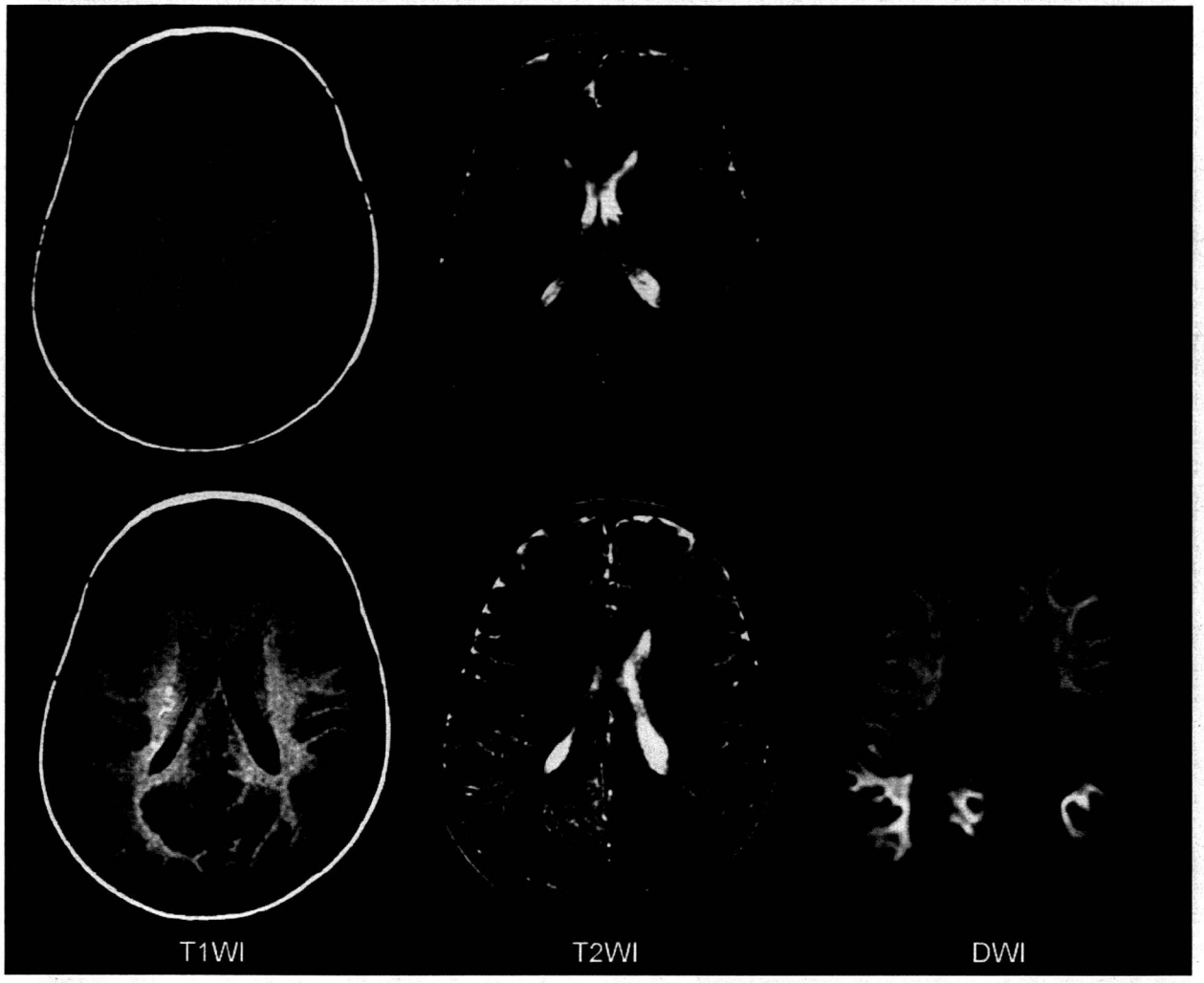

Fig 2. MR imaging findings of a patient with central sparing lesions. Top: Two days after the onset, no abnormalities are observed. Bottom: Four days after the onset, T1-weighted (T1WI) images show unclear gray-white matter differentiation in the bilateral frontal regions. T2-weighted (T2WI) images reveal diffuse thickening of the cortex and increased signal intensities in the bilateral caudate nuclei. Reduced diffusivity is observed in the bilateral frontal and parietooccipital regions on DWIs.

Cognitive impairment was assessed in all surviving patients 1–1.5 years after discharge. Cognitive impairment was usually measured by using the Kaufman Assessment Battery for Children, though it could not be applied in some patients with severe cognitive impairment. The severity of cognitive impairment was defined as mild when the patient's intelligence quotient (IQ) or development quotient (DQ) was between 50 and 70, moderate when IQ/DQ was between 30 and 50, and severe when IQ/DQ was below 30.

Statistical analyses between the 2 groups were performed by using the Mann-Whitney *U* test for numeric variables and the Fisher exact probability test for categoric variables. The outcome of patients was also analyzed by using the Mann-Whitney *U* test. *P* values $< .05$ were statistically significant.

Results

Patient Characteristics

Five boys and 4 girls were analyzed. The median age was 17 months (range, 3–66 months), and 6 of the children were 18 months of age or younger. One patient showed multiple congenital anomalies and developmental delay of unknown cause. Another had a history of febrile seizures. Five patients showed diffuse lesions, and 4 showed central-sparing lesions.

Patient characteristics are summarized in Table 1. Age and sex did not differ between groups. Prodromal illnesses were variable: Virologically proved influenza was observed in 3 patients; exanthem subitum, in 1; gastroenteritis, in 2; and nonspecific febrile illness, in 3.

Neurologic symptoms are also shown in Table 1. Coma was observed within 24 hours after onset in all patients with diffuse lesions. One patient with central-sparing lesions became comatose on the fourth day of illness. Coma was significantly more common in patients with diffuse lesions than in those with central-sparing lesions ($P = .048$). In contrast, a biphasic clinical course was more common in patients with central-sparing lesions than in those with diffuse lesions ($P = .048$). All patients with central-sparing lesions showed a biphasic clinical course. The reduction of consciousness was mild within the first few days after onset, followed by seizures appearing 3–6 days after onset in association with deteriorated consciousness. One patient with diffuse lesions also showed a

Table 1: Patients' characteristics, neurologic symptoms, and outcome

	Diffuse Lesions (n = 5)	Central-Sparing Lesions (n = 4)	P Value
Age (months)*	18 (3–52)	15 (10–66)	NS
Sex (M-F)	3:2	2:2	NS
Prodromal illness			Not done
Influenza	2	1	
Subitum	0	1	
Gastroenteritis	2	0	
NSFI	1	2	
Coma	5	1	.048
Biphasic clinical course	1	4	.048
Seizure at onset	3	4	NS
Prolonged seizure at onset	1	1	NS
Seizure after the first 24 hours	2	4	NS
Outcome			.056
Death	3	0	
Severe cognitive impairment	1	1	
Mild cognitive impairment	1	2	
Healthy	0	1	

Note:—NSFI indicates nonspecific febrile illness; NS, not significant.
* Data are shown as median (range).

biphasic clinical course. In this patient, coma without seizures was the initial presentation, but the reduction of consciousness became milder thereafter. Clustered seizures and worsening of consciousness were observed 2 days after onset. Seizures at onset or after the first 24 hours were observed in all patients with central-sparing lesions, whereas seizures were observed in 3 patients at onset and in 2 after the first 24 hours among those with diffuse lesions. A prolonged seizure was observed in 1 patient with diffuse lesions and in 1 with central-sparing lesions. The duration of seizures was 60 minutes in these patients.

Statistical analyses showed marginal differences in outcome between patients with diffuse-versus-central-sparing lesions (Table 1). All except 1 patient with diffuse lesions died or had severe cognitive impairment, whereas all patients with central-sparing lesions survived and only 1 showed severe cognitive impairment (P = .056). Postmortem examination was not performed in those who died.

Laboratory Data

Maximal AST, ALT, and creatinine kinase levels were significantly higher in patients with diffuse lesions than in those with central-sparing lesions (Table 2). Although abnormalities in platelet counts and lactate dehydrogenase, blood urea nitrogen, and creatinine levels tended to be more severe in patients with diffuse lesions, these differences were not statistically significant. Elevation in ammonia levels, if present, was mild. Hyperglycemia (serum glucose >200 mg/dL) tended to be more common in patients with diffuse lesions, though this difference did not reach statistical significance. CSF analyses did not reveal pleocytosis or increased protein levels in any patient. Disseminated intravascular coagulation was observed in only 1 patient with diffuse lesions. Metabolic acidosis was observed in all except 1 patient with diffuse lesions and in none of those with central-sparing lesions (P = .048).

Neuroimaging Findings

MR imaging during the acute phase (within the first 72 hours after onset) was obtained in 2 patients with diffuse lesions and in 2 with central-sparing lesions. In 2 of 3 patients with diffuse lesions, reduced diffusion was observed in the cortical and subcortical areas in the bilateral frontal and occipital areas (Fig 1). In addition, T1-weighted images demonstrated mild thickening of the cerebral cortex in the corresponding areas, and T2-weighted images revealed mildly increased intensities in the same areas. However, no abnormalities were observed in the remaining 3 patients.

During the subacute phase (from the fourth to the 12th day of illness), MR imaging demonstrated abnormal findings in all patients. As used in the categorization of the patients, markedly reduced diffusion and edematous changes in the entire cortical and subcortical areas were observed in 5 patients (Fig 1). Thickening of the cortex and T1 and T2 prolongation in the subcortical white matter were more remarkable compared with these findings during the acute period in all patients. Blurring of the gray-white matter junction was also prominent. In this group of patients, MR imaging was performed on the fourth day of illness in 1 patient, on the sixth in 2, on the eighth in 1, and on the 12th in 1. In 4 patients with central-sparing lesions, pre- and postcentral areas were clearly spared (Fig 2). Thickening of the cortex and T1 and T2 prolongation in the subcortical white matter were relatively mild, and blurring of the gray-white matter junction was not observed. In this group of patients, MR imaging was performed on the fifth day of illness in 1 patient, on the sixth in 1, on the eighth in 1, and on the 12th in 1.

During the late phase (>2 weeks after onset), MR imaging was conducted in all 7 surviving patients. Three of 5 patients with diffuse lesions survived. Marked cerebral atrophy was observed in 2 patients, and mild cerebral atrophy, in 1 patient on MR imaging during the late phase. Laminar necrosis and increased signal intensities in the subcortical white matter on T2-weighted images were observed in all of these patients. All 4 patients with central-sparing lesions survived. Late MR imaging revealed mild cerebral atrophy in 3 patients and no abnormality in 1. Laminar necrosis was not observed in any patient with central-sparing lesions, whereas mildly increased signal intensities in the subcortical white matter on T2-weighted images were recognized in 3 patients.

No patient showed markedly reduced diffusion in the basal ganglia, thalami, or corpus callosum throughout the clinical course. However, T2-weighted images showed increased signal intensities in the bilateral caudate nuclei in 2 patients with central-sparing lesions during the subacute period.

Discussion

This study demonstrated that acute encephalopathy with reduced diffusion in the bilateral hemispheres can be divided into 2 distinct groups according to the distribution of brain lesions: diffuse and central-sparing lesions. Clinical manifestations, laboratory data, and outcomes were markedly different between patients with diffuse-versus-central-sparing lesions. These results indicate that these 2 groups should be distinguished, though they share common MR imaging abnormalities (ie, widespread reduced diffusion in the cortex and/or subcortical white matter of the bilateral hemispheres).

Patients with diffuse lesions appear to represent a severe phenotype of acute encephalopathy. Clinical symptoms were characterized by rapid and severe deterioration of conscious-

Table 2: Laboratory data

	Diffuse Lesions (n = 5)	Central Sparing Lesions (n = 4)	P Value
Minimal Plt ($\times 10^4/\mu L$)*	14.3 (6.2–36.6)	17.8 (11.3–46.9)	NS
Maximal AST (IU/L)*	917 (189–4407)	107 (53–239)	.028
Maximal ALT (IU/L)*	403 (48–3200)	33 (19–77)	.028
Maximal LDH (IU/L)*	1325 (681–7758)	815 (351–1193)	NS
Maximal CK (IU/L)*	6500 (2057–128472)	320 (62–915)	.014
Maximal BUN (mg/dL)*	19 (7.0–79.1)	12.5 (8.3–15.2)	NS
Maximal Cr (mg/dL)*	0.59 (0.20–2.2)	0.29 (0.22–0.40)	NS
Maximal ammonia (μg/dL)*	147 (35–176)	83 (55–111)	NS
Blood glucose >200 mg/dL	4	1	NS
CSF cell >10/μL	0	0	NS
CSF protein >40 mg/dL	0	0	NS
DIC	1	0	NS
Metabolic acidosis	4	0	.048

Note:—Plt indicates platelet counts; LDH, lactate dehydrogenase; CK, creatinine kinase; BUN, blood urea nitrogen; Cr, creatinine; DIC, disseminated intravascular coagulation; AST, aspartate aminotransferase; ALT, alanine aminotransferase.
* Data are shown as median (range).

ness, though seizures were not always observed. A biphasic clinical course was rare. Laboratory abnormalities were prominent, including elevated AST, ALT, and creatinine kinase levels; hyperglycemia; and metabolic acidosis. The outcome for patients with diffuse lesions was very poor. Death or severe neurologic sequelae were observed in 4 of 5 patients. These findings may be explained by a systemic inflammatory response, in which multiple organ failure, shock, and disseminated intravascular coagulation are often observed. During the acute stage of acute encephalopathy, the serum and CSF levels of inflammatory cytokines, such as interleukin-6 and tumor necrosis factor-α, were markedly elevated.[7-9] Several pathologic studies have suggested that vascular injury as a result of endothelial damage by inflammatory cytokines is the pathologic substrate of severe types of acute encephalopathy, such as acute necrotizing encephalopathy.[1,10] Although serum and CSF levels of inflammatory cytokines were not measured, it is possible that hypercytokinemia may contribute to the pathogenesis of diffuse lesions.

In contrast, patients with central-sparing lesions appear to represent a relatively mild phenotype of acute encephalopathy. Coma was uncommon and laboratory abnormalities were mild, if present. No patient died, though various degrees of cognitive impairment were observed as neurologic sequelae. A biphasic clinical course is characteristic of this group of patients, as described previously.[3] Several studies on acute encephalopathy have also reported a biphasic clinical course.[11-14] Onset is often marked by a prolonged seizure followed by improved consciousness. However, clustered seizures, signs of frontal lobe dysfunction, and worsening of consciousness become apparent at 3–4 days after onset. These features were observed in our patients with central-sparing lesions. The pathogenesis of acute encephalopathy with central-sparing lesions may be different from that of acute encephalopathy with diffuse lesions. Some authors have suggested that this subtype of acute encephalopathy is caused by excitotoxicity,[3,15] because prolonged seizures are often observed at the onset of AESD. MR spectroscopy has shown increased glutamate concentrations and decreased N-acetylaspartate levels in patients with AESD.[16] However, a prolonged seizure at onset was rare in our patients. Further studies are necessary to clarify the pathogenesis of acute encephalopathy with central-sparing lesions.

We consider it possible to distinguish central-sparing lesions from frontal occipital lesions, which may precede diffuse lesions. First, the appearance of reduced diffusion is earlier in frontal occipital lesions than in central-sparing lesions. In this study, central-sparing lesions were not observed in any patient within the first 3 days after onset, consistent with several previous reports.[3,12-14,17] In contrast, frontal occipital lesions were recognized within the first 3 days after onset and were followed by diffuse lesions. Second, the distribution of brain lesions is different in the 2 situations. In patients with central-sparing lesions, the areas without reduced diffusion were strictly limited, around the Sylvian fissures. In the occipital lobes, lesions in the lateral areas were more prominent than those in the mesial areas. In contrast, lesions were located in the anterior half of the frontal lobes and mesial areas of the occipital lobes. Diffusion abnormalities were absent in the posterior half of the frontal lobes and the parietotemporal lobes and were less prominent in the lateral areas of the occipital lobes. However, these observations were based on a small number of patients.

The results of our study are not conclusive. Neuroimaging evaluations of many patients will be necessary to clarify differences between central-sparing lesions and frontal occipital lesions. The recognition of frontal-occipital lesions is useful in the early diagnosis of acute encephalopathy with diffuse lesions and may contribute to early intensive treatment. Our previous study indicated that early steroid use was related to better outcomes in children with acute necrotizing encephalopathy without brain stem lesions.[18]

The DWI patterns of our patients were characteristic, though reduced diffusion in the bilateral hemispheres may be observed with other causes of brain injury, such as hypoxic-ischemic encephalopathy and shaken infant syndrome.[19,20] It is possible that encephalopathy due to substance abuse or intoxication may exhibit similar DWI abnormalities. Thus, the distinction between acute encephalopathy and brain injuries due to other causes may be problematic solely on the basis of imaging findings. For this reason, a diagnosis should be made only after considering clinical manifestations, physical and

neurologic examinations, and laboratory data, in combination with MR imaging abnormalities. In our patients, there was no evidence of hypoxia-ischemia, nonaccidental head injury, or substance intoxication.

To our knowledge, the subtypes of acute encephalopathy have not been sufficiently established at present. The clinical presentation and imaging features of our patients overlap partly with other acute encephalopathy syndromes, including AESD,[3] acute infantile encephalopathy predominantly affecting the frontal lobes,[11] human herpes virus-6 encephalopathy with clusters of convulsions during the eruptive stage,[12] and subacute encephalopathy.[14] These acute encephalopathy syndromes likely represent a spectrum of disorders that share a common process in terms of brain injury. Multidisciplinary studies and further clinical experience are required to clarify the relationships between these syndromes.

In conclusion, acute encephalopathy with reduced diffusion in the bilateral hemispheres can be divided according to the pattern of brain lesions. Patients with diffuse lesions were characterized by coma, severe abnormalities in laboratory test results, and poor neurologic outcome, whereas those with central-sparing lesions were characterized by a biphasic clinical course, less severe abnormalities on laboratory test results, and relatively mild neurologic sequelae. Further neuroimaging studies with larger numbers of patients are necessary to establish the subtypes of MR imaging for acute encephalopathy with reduced diffusion in the bilateral hemispheres and will contribute to clarifying its pathogenesis and effective treatments.

References

1. Mizuguchi M, Abe J, Mikkaichi K, et al. **Acute necrotising encephalopathy of childhood: a new syndrome presenting with multifocal, symmetric brain lesions.** *J Neurol Neurosurg Psychiatry* 1995;58:555–61
2. Tada H, Takanashi J, Barkovich AJ, et al. **Clinically mild encephalitis/encephalopathy with a reversible splenial lesion.** *Neurology* 2004;63:1854–58
3. Takanashi J, Oba H, Barkovich AJ, et al. **Diffusion MRI abnormalities after prolonged febrile seizures with encephalopathy.** *Neurology* 2006;66:1304–09
4. Takanashi J, Tsuji M, Amemiya K, et al. **Mild influenza encephalopathy with biphasic seizures and late reduced diffusion.** *J Neurol Sci* 2007;256:86–89
5. Traul DE, Traul CS, Matsumoto J, et al. **Acute encephalopathy with biphasic seizures and late restricted diffusion on MRI in a Japanese child living in the USA.** *Dev Med Child Neurol* 2008;50:717–19
6. Nagao T, Morishima T, Kimura H, et al. **Prognostic factors in influenza-associated encephalopathy.** *Pediatr Infect Dis J* 2008;27:384–89
7. Ichiyama T, Endo S, Kaneko M, et al. **Serum cytokine concentrations of influenza-associated acute necrotizing encephalopathy.** *Pediatr Int* 2003;45:734–36
8. Ichiyama T, Isumi H, Ozawa H, et al. **Cerebrospinal fluid and serum levels of cytokines and soluble tumor necrosis factor receptor in influenza virus-associated encephalopathy.** *Scand J Infect Dis* 2003;35:59–61
9. Aiba H, Mochizuki M, Kimura M, et al. **Predictive value of serum interleukin-6 level in influenza virus-associated encephalopathy.** *Neurology* 2001;57:295–99
10. Mizuguchi M. **Acute necrotizing encephalopathy of childhood: a novel form of acute encephalopathy prevalent in Japan and Taiwan.** *Brain Dev* 1997;19:81–92
11. Yamanouchi H, Kawaguchi N, Mori M, et al. **Acute infantile encephalopathy predominantly affecting the frontal lobes.** *Pediatr Neurol* 2006;34:93–100
12. Nagasawa T, Kimura I, Abe Y, et al. **HHV-6 encephalopathy with cluster of convulsions during eruptive stage.** *Pediatr Neurol* 2007;36:61–63
13. Okamoto R, Fujii S, Inoue T, et al. **Biphasic clinical course and early white matter abnormalities may be indicators of neurological sequelae after status epilepticus in children.** *Neuropediatrics* 2006;37:32–41
14. Okumura A, Kidokoro H, Itomi K, et al. **Subacute encephalopathy: clinical features, laboratory data, neuroimaging, and outcomes.** *Pediatr Neurol* 2008;38:111–17
15. Mizuguchi M, Yamanouchi H, Ichiyama T, et al. **Acute encephalopathy associated with influenza and other viral infections.** *Acta Neurol Scand* 2007(suppl);186:45–56
16. Takanashi J, Tada H, Terada H, et al. **Excitotoxicity in acute encephalopathy with biphasic seizures and late reduced diffusion.** *AJNR Am J Neuroradiol* 2009;30:132–35. Epub 2008 Aug 13
17. Tada H, Takanashi JI, Terada H, et al. **Severe form of acute influenza encephalopathy with biphasic seizures and late reduced diffusion.** *Neuropediatrics* 2008;39:134–36
18. Okumura A, Mizuguchi M, Kidokoro H, et al. **Outcome of acute necrotizing encephalopathy in relation to treatment with corticosteroids and gammaglobulin.** *Brain Dev* 2009;31:221–27. Epub 2008 May 5
19. Biousse V, Suh DY, Newman NJ, et al. **Diffusion-weighted magnetic resonance imaging in shaken baby syndrome.** *Am J Ophthalmol* 2002;133:249–55
20. Barkovich AJ. **Brain and spine injuries in infancy and childhood.** In: Barkovich AJ, ed. *Pediatric Neuroimaging*. 4th ed. Philadelphia: Lippincott Williams & Wilkins; 2005:190–290

JOURNAL OF CLINICAL MICROBIOLOGY, Jan. 2010, p. 57–63 Vol. 48, No. 1
0095-1137/10/$12.00 doi:10.1128/JCM.00698-09

Rapid and Specific Detection of Amantadine-Resistant Influenza A Viruses with a Ser31Asn Mutation by the Cycling Probe Method[▽]

Yasushi Suzuki,* Reiko Saito, Hassan Zaraket, Clyde Dapat, Isolde Caperig-Dapat, and Hiroshi Suzuki

Department of Public Health, Graduate School of Medical and Dental Sciences, Niigata University, Niigata, Japan

Received 6 April 2009/Returned for modification 17 June 2009/Accepted 28 October 2009

Amantadine is one of the antiviral agents used to treat influenza A virus infections, but resistant strains have widely emerged worldwide. In the present study, we developed a novel method to detect amantadine-resistant strains harboring the Ser31Asn mutation in the M2 gene based on the cycling probe method and real-time PCR. We also studied the rate of amantadine resistance in the 2007–2008 influenza season in Japan. Two different primer and cycling probe sets were designed for A/H1N1 and A/H3N2 each to detect a single nucleotide polymorphism corresponding to Ser/Asn at residue 31 of the M2 protein. By using nasopharyngeal swabs from patients with influenza-like and other respiratory illnesses and virus isolates, the specificity and the sensitivity of the cycling probe method were evaluated. High frequencies of amantadine resistance were detected among the A/H1N1 (411/663, 62%) and A/H3N2 (56/56, 100%) virus isolates collected from six prefectures in Japan in the 2007–2008 influenza season. We confirmed that the cycling probe method is suitable for the screening of both nasopharyngeal swabs and influenza virus isolates for amantadine-resistant strains and showed that the incidence of amantadine resistance among both A/H1N1 and A/H3N2 viruses remained high in Japan during the 2007–2008 season.

Adamantanes (amantadine and rimantadine) have been used for the prevention and treatment of influenza A virus infections (25). The molecular basis of resistance has been identified as single nucleotide changes that lead to corresponding amino acid substitutions at one of four critical amino acid residues (residues 26, 27, 30, and 31) in the transmembrane region of the M2 ion channel protein (19, 26, 27). Recent studies suggest that the rates of influenza virus A/H3N2 resistance to amantadine and rimantadine have been high globally since 2005 (2, 6, 7, 9, 29, 30), while the rates of resistance among A/H1N1 viruses varied from country to country but increased sharply from 2006 onwards (1, 9, 32). It should be noted that resistance in both subtypes was almost exclusively associated with one amino acid substitution at residue 31 (Ser to Asn) of the M2 ion channel protein after 2005 (1, 2, 6, 7, 9, 29, 30, 32).

We have previously established methods for the detection of amantadine susceptibility, such as the virus titration method with comparison of the 50% tissue culture infectious doses ($TCID_{50}$s; $TCID_{50}$/0.2 ml) in the presence and the absence of amantadine (24) and PCR-restriction fragment length polymorphism (PCR-RFLP) analysis (21, 31). Other methods for the detection of resistant strains have also been reported, such as enzyme-linked immunosorbent assay (ELISA) (4), plaque reduction assay (13), and DNA sequencing (24). In general, however, conventional methods are time-consuming. Recently, a high-throughput method of genetic analysis called pyrosequencing was used as a rapid method for screening for amantadine and neuraminidase inhibitor resistance (6–9, 11); however, the cost of pyrosequencing is not always coverable for every laboratories.

In the study described here, we developed a rapid assay using a chimera probe-adapted real-time PCR, or the cycling probe method, to detect amantadine-resistant viruses with the Ser31Asn substitution in the M2 ion channel protein. Furthermore, we report the frequency of amantadine resistance among influenza A viruses in six prefectures in Japan in the 2007–2008 influenza season.

MATERIALS AND METHODS

Design of cycling probes. The cycling probe technology is a unique nucleic acid-based method that detects single nucleic acid polymorphisms (SNPs) in a target DNA sequence by using a probe-adapted real-time PCR (3, 10) (Fig. 1). The cycling probe method involves a reaction between a chimeric fluorescence- and quencher-labeled DNA/RNA oligonucleotide probe (cycling probe) and RNase (RNase H). This cycling probe is a short DNA fragment (normally 10- to 20-mer) accommodating an RNA complementary to the nucleotide of interest that undergoes degeneration by RNase H activity, once a DNA-RNA complex is formed during annealing. This degeneration leads to the emission of strong fluorescence (17), and by measuring the intensity of the fluorescence, the amount of amplified product can be quantified (Fig. 1a). For SNP typing, two cycling probes labeled with two different fluorescence dyes (6-carboxyfluorescein [FAM] or 6-carboxy-X-rhodamine [ROX]) are used, with each probe harboring RNA corresponding to the wild-type nucleotide or the nucleotide with a mutation at the SNP position (Fig. 1b).

RNA extraction and reverse transcription. Nasopharyngeal swab samples that previously tested positive for influenza virus by virus isolation and for which their genetic substitution of interest was confirmed by sequencing were selected for evaluation of the assay's specificity. These included 20 amantadine-sensitive and 20 amantadine-resistant samples each of the influenza virus A/H1N1 and A/H3N2 subtypes. The viral RNA of influenza viruses A/H1N1 and A/H3N2 and other common respiratory viruses (respiratory syncytial virus, parainfluenza virus, enterovirus, and rhinovirus) and the DNA of adenovirus were extracted from 100 μl of the supernatants of the nasopharyngeal swabs or the virus culture supernatant by using an Extragen II kit (Kainos, Tokyo, Japan), according to the manufacturer's instructions. Reverse transcription was performed in a reaction separate from the real-time PCR in order to obtain 25 μl of the first-strand cDNA of the influenza virus genome by using influenza A virus universal primer Uni12, as reported elsewhere (16). The RNA of the other respiratory viruses

* Corresponding author. Mailing address: Department of Public Health, Niigata University, Graduate School of Medical and Dental Sciences, 1-757, Asahimachi-Dori, Niigata City, Niigata Prefecture 951-8510, Japan. Phone: 81-25-227-2129. Fax: 81-25-227-0765. E-mail: yasshi@med.niigata-u.ac.jp.

▽ Published ahead of print on 4 November 2009.

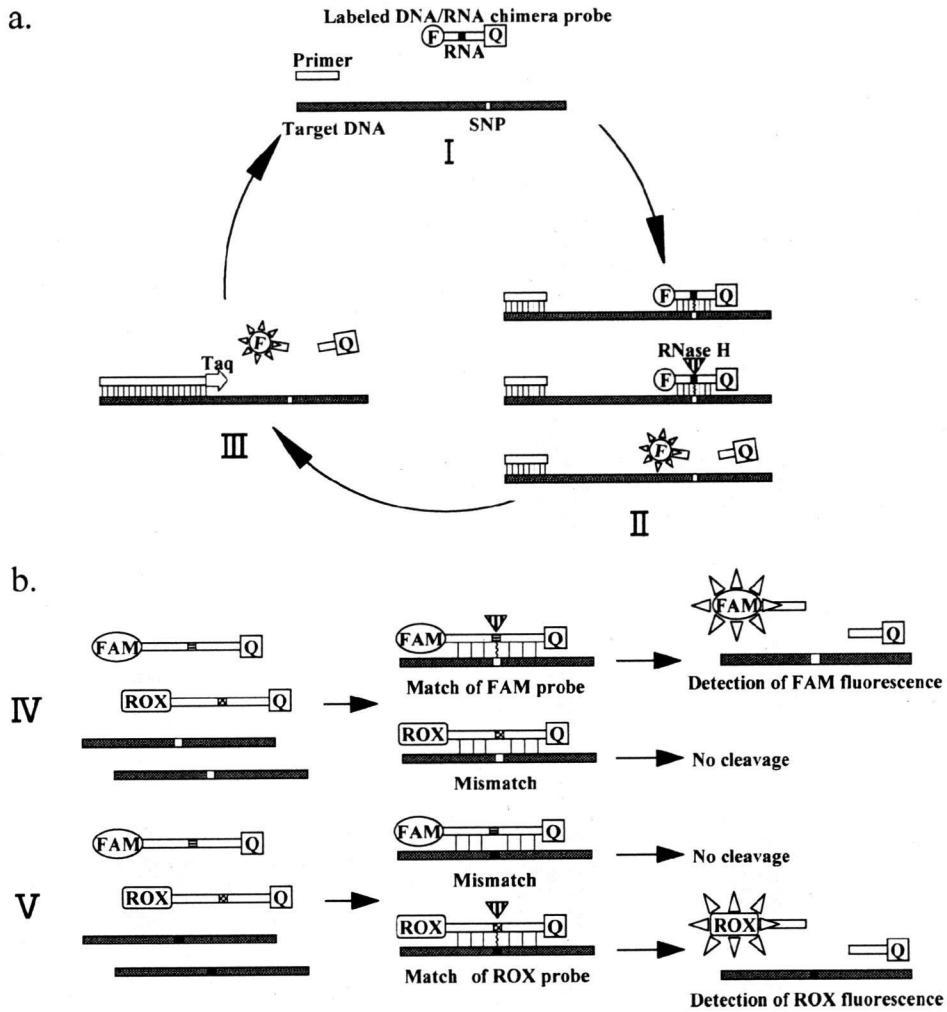

FIG. 1. Illustration of cycling probe technology using real-time PCR for SNP typing. F and Q represent fluorescence and quencher, respectively. (a) I, denaturation of target DNA; II, primer annealing and prove hybridization and then cleavage by RNase H; III, extension of target DNA by *Taq* polymerase and detection of fluorescence. (b) Each probe detects SNP in the matched sequence; IV, FAM-labeled probe matches target DNA and is cleaved to release the FAM fluorescence by RNase H; V, ROX-labeled probe matched target DNA and is cleaved by RNase H to release the ROX fluorescence.

used to check for cross-reactions was reverse transcribed by using random primers (Invitrogen Corp., Carlsbad, CA).

Primers, probes, and PCR conditions. PCR primers (sets of forward and reverse primers for H1N1 and H3N2) were designed to specifically amplify the M2 gene transmembrane region of influenza viruses A/H1N1 and A/H3N2; the PCR product sizes were 155 bp and 98 bp, respectively. The chimera probes H1N1-AS (where AS indicates amantadine sensitive), H1N1-AR (where AR indicates amantadine resistant), H3N2-AS, and H3N2-AR were created to detect Ser31 (AGT) and Asn31(AAT) in the M2 gene, respectively (the underscores indicate the nucleotide replaced by RNA) (TaKaRa Bio Inc.) (Table 1). A CycleavePCRCore kit (TaKaRa Bio Inc.) was used for the PCR and the simultaneous cleavage of RNase H. The amplification was carried out in a total volume of 25 μl. The reaction mixture contained (final concentrations are given) 1× CycleavePCR buffer, 3 mM Mg^{2+}, 0.3 mM each deoxynucleoside triphosphates, 5 pmol of each PCR primer (forward and reverse), 5 pmol of each probe (the FAM-labeled probe and the ROX-labeled probe), 100 U of *Tli* RNase HII, and 1.25 U of Ex *Taq* HS (TaKaRa Bio Inc.). One microliter of cDNA was added to the reaction mixture as the DNA template. To detect A/H1N1 viruses, a set of primers and probes consisting of the H1N1 forward primer, the H1N1 reverse primer, and the H1N1-AS and H1N1-AR probes was used; and to detect A/H3N2 viruses, a relevant set of H3N2 primers and probes was employed (Table 1). PCR amplification and fluorescence detection were performed with a TP800 thermal cycler Dice real-time PCR system (TaKaRa Bio Inc.). The conditions of the PCR cycles were as follows: a hold at 95°C for 10 s, followed by 40 cycles of denaturation at 95°C for 5 s, primer annealing at 57°C for 10 s, and extension and emission of fluorescence at 72°C for 15 s. Duplicate wells were used for each sample, and amantadine-sensitive (Ser31) and -resistant (Asn31) control plasmids were included in each run in a 96-well plate.

Control plasmids. Four positive control plasmids, H1N1-AS, H1N1-AR, H3N2-AS, and H3N2-AR, were made from the PCR product of each subtype amplified with the same PCR primers used in this study. Both the H1N1-AS and H3N2-AS controls contained sequences that code for serine at position 31 (amantadine sensitive), while the H1N1-AR and H3N2-AR controls possessed sequences with mutations that code for asparagine at position 31. The purified PCR product was ligated and cloned into a pMD20-T vector (TaKaRa Bio Inc.) and was transformed into JM109 competent cells (TaKaRa Bio Inc.) with a Mighty TA cloning kit (TaKaRa Bio Inc.), according to the manufacturer's instructions. Positive clones were selected by the blue-white colony pickup method and were then cultured in Luria-Bertani broth and incubated overnight at 37°C in a shaking incubator. The bacterial culture was pelleted by centrifugation, and the plasmids were extracted with a Wizard Plus SV Minipreps DNA purification system (Promega, Madison, WI), according to the manufacturer's instructions. Sequencing was performed with an ABI Prism BigDye Terminator (version 3.1) cycle sequencing kit (Applied Biosystems, Foster City, CA), ac-

TABLE 1. Primers and probes used for real-time PCR

Subtype	Primers and probes	Sequence (5′–3′)	Location[a]
H1N1	H1N1 forward primer	5′-GCTCTAGCACTGGTCTGAAA-3′	696–715
	H1N1 reverse primer	5′-AGGCGATCAATAATCCACAA-3′	831–850
	H1N1-AS probe[b]	5′-(FAM[c])-TGCCGCAA*G*TA-(Eclipse[d])-3′	797–807
	H1N1-AR probe[b]	5′-(ROX[c])-TGCCGCAA*A*TA-(Eclipse[d])-3′	797–807
H3N2	H3N2 forward primer	5′-AGACCTATCAGAAACGAATG-3′	738–757
	H3N2 reverse primer	5′-CACAGTATCAAGTGCAAG-3′	818–835
	H3N2-AS probe[b]	5′-(FAM[c])-TGCTGCGA*G*TA-(Eclipse[d])-3′	796–807
	H3N2-AR probe[b]	5′-(ROX[c])-TTGCTGCGA*A*TA-(Eclipse[d])-3′	796–807

[a] Location of primers and probes in the M gene (total length, 1,027 bp), segment 7, of influenza A virus.
[b] Fluorescent dye- and quencher-labeled DNA-RNA chimeric probe. The boldface italic letters in the sequences of these probes indicate the nucleotide replaced by RNA.
[c] Fluorescent molecules.
[d] Quenching molecule.

cording to the manufacturer's instructions, and the products were sequenced with an ABI 3100 automatic sequencer (Applied Biosystems) to confirm the presence of the insert. The sequences were aligned and compiled by using BioEdit software (version 7.0.7) (14).

After the DNA concentrations of the plasmids with the wild-type and mutant sequences were measured with a spectrophotometer (GeneQuant 1300; GE Healthcare UK Ltd., Buckinghamshire, England), serial 10-fold dilutions were made to determine the detection sensitivities of this method for the wild-type and mutant sequences of each subtype. In addition, mixtures of plasmids with the wild-type and mutant sequences were tested at ratios of 1:1, 1:10, 1:100, and 1:1,000 to examine the detection sensitivity of the method with a mixed population.

Prevalence of amantadine resistance in clinical samples. Clinical samples were collected from patients with influenza-like illnesses at 14 outpatient clinics and hospitals from October 2007 to April 2008 in six prefectures (Hokkaido, Niigata, Gunma, Kyoto, Hyogo, and Nagasaki) in Japan. Briefly, after written or oral informed consent was obtained, nasopharyngeal swab specimens were collected from the patients with influenza-like illnesses, and the medication used in the clinic for the treatment of influenza (amantadine, oseltamivir, or zanamivir) was recorded. The swabs were stored in viral transport medium and were kept at 4°C until transportation to the Department of Public Health, Niigata University, for virus isolation within 1 week. Then, 100-μl aliquots of supernatants of the nasopharyngeal swab specimens were inoculated into Madin-Darby canine kidney cells (MDCK), prepared in 48-well plates. The plates were incubated at 34°C under a 5% CO_2 atmosphere for up to 10 days to assess the samples for the presence of cytopathic effects (CPE). Fifty-microliter aliquots of the supernatants of CPE-positive samples were then passaged twice to obtain a sufficient virus titer for virus identification. The influenza virus isolates were typed and subtyped by a hemagglutination inhibition (HAI) assay with commercially available antisera to the influenza virus vaccine strain for the 2007–2008 season in Japan (Denka Seiken Co., Ltd., Tokyo, Japan), namely, A/Solomon Islands/3/2006 (A/H1N1), A/Hiroshima/52/2005 (A/H3N2), and B/Malaysia/2506/2004, and with guinea pig red blood cells. RNA extraction, cDNA synthesis, and the cycling probe real-time PCR were employed with the nasopharyngeal swab specimens and virus isolates as described above to examine whether they possessed the S31N substitution.

RESULTS

Establishment of cycling probe method. A FAM-labeled cycling probe was designed to detect the sequence for amantadine sensitivity (AGT) at amino acid position 31 in the M2 protein by replacing guanine DNA with RNA, while the ROX probe replaced the adenine DNA with RNA corresponding to the sequence for amantadine resistance (AAT) (Table 1). If the sample in question had a sequence conferring sensitivity, the fluorescent emission of FAM was detected after the hybridized RNA and DNA complex at the guanine position was degenerated by RNase H and the dye was subsequently liberated from the quencher. The same reaction occurred with the sequence conferring amantadine resistance, which harbored adenine at the identical position (position 31) and which is reported by the detection of ROX.

The cycling probes were first tested with DNA plasmids with the known wild-type and mutant sequences in the M2 protein for both subtype A/H1N1 and subtype A/H3N2, which served as controls for our two-step cycling probe real-time PCR. Fluorescence intensities with threshold cycle (C_T) values of between 16 and 20 for 2.9×10^7 copies for A/H1N1 and 2.95×10^7 copies for A/H3N2 were detected for the plasmids with the wild-type sequence and the plasmids with the mutant sequence (Fig. 2a and b). The detection limits for the controls were 2.9×10^2 copies for the A/H1N1 plasmid and 2.95×10^2 copies for the A/H3N2 plasmid, giving C_T values of about 38 (Fig. 2c and d).

The study of mixtures of control plasmids with the wild-type and mutant sequences showed that the cycling probes gave C_T values with each dye in a plasmid concentration-dependent manner. A ratio of 1:1 gave similar C_T values for both the wild-type and the mutant plasmids, and the C_T values gradually increased as the proportion of the wild-type or mutant plasmids became smaller (data not shown). The detection limit was a ratio of 1:100 for the mutant and wild-type plasmids for both subtype H1N1 and subtype H3N2.

We next evaluated the sensitivity and the specificity of the method for the detection of strains previously determined to be amantadine sensitive and resistant using clinical influenza isolates (high template concentration) and nasopharyngeal swab specimens (low template concentration). The H1N1-AS probe successfully detected the amantadine-sensitive virus (Fig. 3a) and the H1N1-AR probe successfully detected the amantadine-resistant virus (Fig. 3b) from both clinical isolates and nasopharyngeal swab specimens. Similar results for the differentiation (specific detection) of sensitive and resistant strains were obtained with A/H3N2 probes and clinical samples of A/H3N2 (Fig. 3c and d). The genetic sequencing results matched the cycling probe results. The average C_T value observed for the isolates was low (15 to 20 cycles) compared with that for the nasopharyngeal swab specimens (25 to 35 cycles). A reaction was considered positive only when the C_T value did not exceed 38 cycles after a 40-cycle PCR run.

We evaluated the specificities of the probes for human influenza virus and other common respiratory viruses (Table 2).

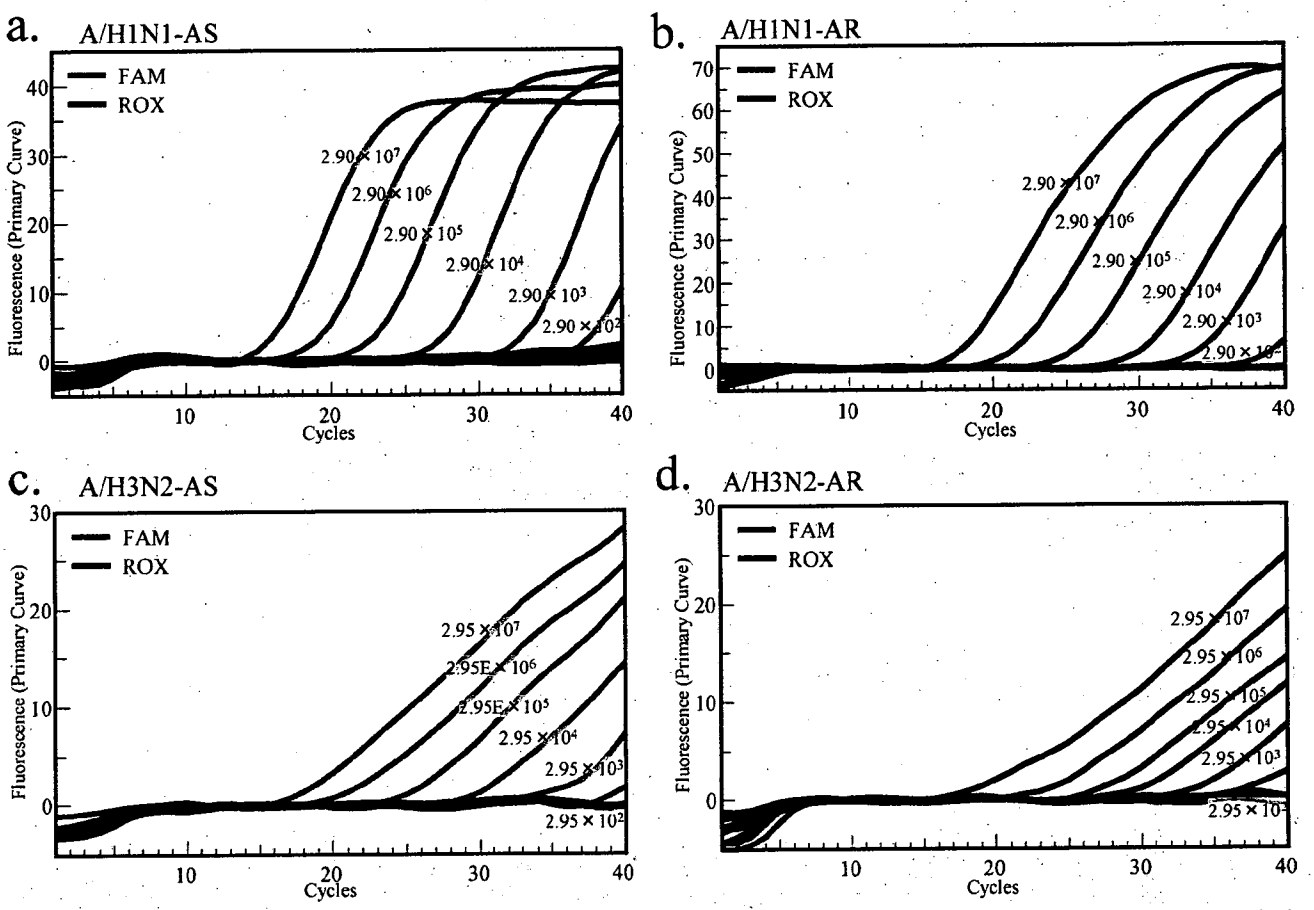

FIG. 2. Testing of serial dilutions of control plasmids with inserts of the M2 gene sequences of influenza A viruses by the cycling probe method. FAM fluorescence was detected with the sequence for amantadine sensitivity (AS; Ser31), and ROX fluorescence was seen with the sequence for amantadine resistance (AR; Asn31). Control plasmids with the A/H1N1 sequences (H1N1-AS and H1N1-AR) reacted with probes H1N1-AS and H1N1-AR, respectively (a and b). Control plasmids with the A/H3N2 sequences (H3N2-AS and H3N2-AR) specifically reacted with the respective A/H3N2 probes (c and d).

The H1N1 probes reacted only with amantadine-sensitive and -resistant A/H1N1 strains and did not react with human influenza virus A/H3N2, whereas the H3N2 probes reacted only with amantadine-sensitive and -resistant A/H3N2 strains and did not react with human influenza virus A/H1N1. Neither probe reacted with samples containing influenza B virus, other respiratory virus-positive samples, or negative (no-template) samples. Furthermore, 99 swab specimens, including 85 isolation-positive samples and 14 isolation-negative samples, were directly tested with the cycling probe. Forty isolates each of H1N1 and H3N2 were identified, and 20 isolates each of amantadine-sensitive and isolation-positive H1N1 and H3N2 strains were also identified by these methods. Neither probe reacted with influenza B viruses, respiratory syncytial virus-positive samples, or isolation-negative samples.

Prevalence of amantadine-resistant influenza viruses in the 2007–2008 season in Japan. A total of 1,027 primary clinical samples were collected from clinicians, and eventually, 756 (73.4%) influenza viruses were isolated by the use of MDCK cells. Of these, 672 (88.9%) isolates were influenza virus A/H1N1, 62 (8.2%) were influenza virus A/H3N2, and 22 (2.9%) were influenza B virus by HAI testing. The cycling probe assay successfully identified 663 (98.7%) of the 672 A/H1N1 viruses and 56 (90.0%) of the 62 A/H3N2 viruses. In this assay, 62.0% (411 of 663) of the A/H1N1 isolates and 100% (56 of 56) of the A/H3N2 isolates were amantadine resistant (Table 3). None of the patients received amantadine before sampling or after diagnosis.

DISCUSSION

We developed a rapid and high-throughput real-time PCR assay for the detection of the Ser31Asn mutation in the M2 gene transmembrane region in both the influenza virus A/H1N1 and the influenza virus A/H3N2 subtypes using specific florescent-labeled chimeric probes. The assay is called the cycling probe technology (3, 10). We demonstrated in the study described here that the method is highly specific for the detection of the SNP for amantadine resistance in the M2 gene and could successfully differentiate the two influenza A virus subtypes. Eventually, we showed a high frequency of occurrence of amantadine-resistant strains of both subtypes during the 2007–2008 season in Japan.

The results of the cycling probe assay described in this paper

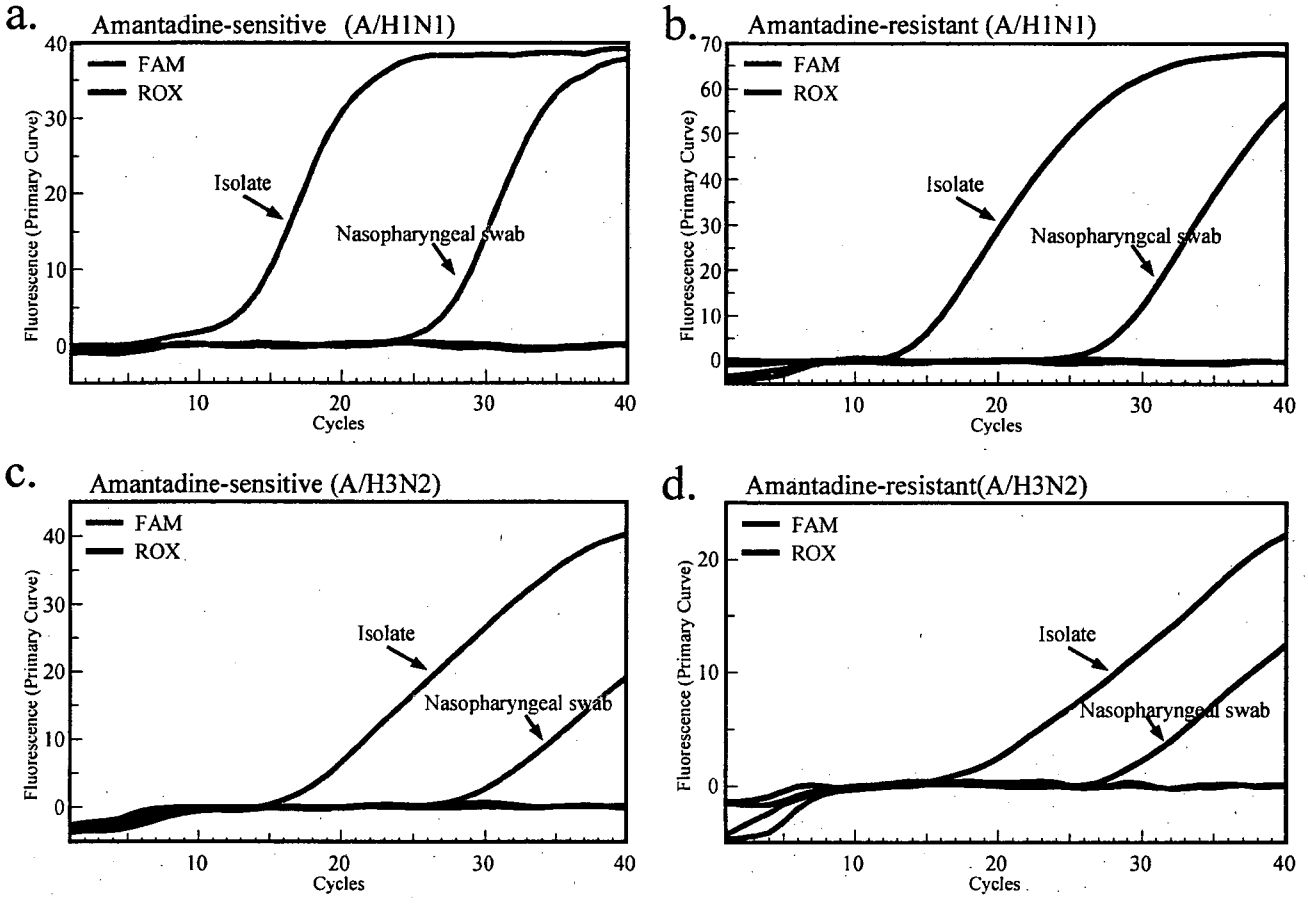

FIG. 3. Detection of amantadine-resistant influenza A virus strains with a mutation at position 31 in the M2 gene by the use of clinical isolates and nasopharyngeal swab specimens. A/H1N1 amantadine-sensitive (a) and amantadine-resistant (b) strains reacted with each of the FAM and the ROX probes. A/H3N2 amantadine-sensitive (c) and amantadine-resistant (d) strains reacted with the specific corresponding probes.

demonstrated agreement with the results of gene sequencing. Virus detection was successful by the use of both nasopharyngeal swabs and virus isolates from clinical samples, despite the differences in the virus concentration between the two types of samples. In addition, the cycling probe sets used to detect both subtypes did not show false-positive reactions with the other influenza A virus subtypes, influenza B virus, or other respiratory viruses. The sensitivity of the method for the detection of influenza virus A/H3N2, based on virus isolation, was lower than that for the detection of A/H1N1, which was due to sporadic nucleotide mismatches in the primers and/or probes for A/H3N2. At present, the proportions of viruses with a mismatch is not sufficiently significant to require a change to the sequence of the primers or the probes. Thus, our method is highly specific and is suitable for the subtyping of human influenza A viruses, along with the identification of amantadine-resistant viruses. In addition, our method successfully detected mixed populations of plasmids with mutant and wild-type sequences at a ratio as low as 1:100. This method can be used to quantify the virus loads in both clinical samples and samples tested in vitro containing a mixed mutant and wild-type virus population.

Most protocols currently employed are based on one-step reverse transcription real-time PCR (22, 33), and thus, it is common to use as the control a known concentration of RNA. However, in the cycling probe method, it is not possible to adopt a one-step real-time PCR, because it includes RNase H and the template could not achieve a sufficient length of cDNA during the reverse transcription. Other common controls are cDNA (two-step method), but plasmid preparations have higher degrees of stability and reproducibility (20, 23, 28).

Various methods has been used to examine virus isolates for their amantadine susceptibilities, such as ELISA (4), plaque reduction assay (13), the $TCID_{50}$/0.2-ml method (24), PCR-RFLP analysis (21, 31), and DNA sequencing (24). However, the time to the retrieval of results by these methods may be from several hours to a few days. The advantage of our approach is that we can detect amantadine-resistant strains directly from patients' nasopharyngeal swab specimens in only 3 h: 1.5 h for RNA extraction and cDNA synthesis and 1.5 h for the real-time PCR run. Our method can be also used for dual subtyping and resistance detection if the two subtype-specific reactions are performed in parallel in a 96-well plate for sample sizes of $\geq$45. Pyrosequencing (6–9, 11) and DNA microarray analysis (34) were recently developed for the detection of amantadine-resistant strains. These methods have high

TABLE 2. Probe reaction performance with various virus samples

Sample type	Virus[a]	Subtype[b]	Susceptibility to amantadine[c]	No. of samples	No. of samples positive with probe set: H1N1 FAM probe	H1N1 ROX probe	H3N2 FAM probe	H3N2 ROX probe
Clinical samples	Influenza A virus	H1N1	Sensitive	4	4	0	0	0
	Influenza A virus	H1N1	Resistant	4	0	4	0	0
	Influenza A virus	H3N2	Sensitive	4	0	0	4	0
	Influenza A virus	H3N2	Resistant	4	0	0	0	4
	Influenza B virus	NA[d]	NA	4	0	0	0	0
	Respiratory syncytial virus	NA	NA	1	0	0	0	0
	Parainfluenza virus	NA	NA	1	0	0	0	0
	Enterovirus	NA	NA	1	0	0	0	0
	Rhinovirus	NA	NA	2	0	0	0	0
	Adenovirus	NA	NA	1	0	0	0	0
Nasopharyngeal swab	Influenza A virus	H1N1	Sensitive	20	20	0	0	0
	Influenza A virus	H1N1	Resistant	20	0	20	0	0
	Influenza A virus	H3N2	Sensitive	20	0	0	20	0
	Influenza A virus	H3N2	Resistant	20	0	0	0	20
	Influenza B virus	NA	NA	5	0	0	0	0
	Negative sample	NA	NA	10	0	0	0	0
	Respiratory syncytial virus	NA	NA	4	0	0	0	0

[a] Viruses were initially detected by virus isolation and PCR with specific primers.
[b] Typed and subtyped by hemagglutinin inhibition assay with vaccine strain antisera.
[c] Resistant strains of both subtypes had a serine-to-asparagine change in residue 31 of the M2 ion channel protein.
[d] NA, not addressed.

throughputs and are rapid, just as our cycling probe technique is, but unlike our method, they have the disadvantage of the costs for the machine and the reagents, which are too high for their routine use in laboratories. Thus, our method is perhaps one of the quickest and most affordable with respect to the running cost (which is equivalent to that of the TaqMan probe method) among the methods currently available for the identification of amantadine resistance, and it is ideal for large-scale screening for resistant mutants and subtyping even with specimens with low template concentrations, such as nasopharyngeal swab specimens. Of note, the TaqMan probe real-time PCR was applied for the detection of oseltamivir-resistant influenza virus A/H1N1 possessing His274Tyr (N2 numbering) in the neuraminidase gene and used for monitoring for resistant viruses (5). We are currently developing new cycling probe sets to detect other amantadine resistance mutations in the M2 gene and the oseltamivir resistance mutation (His274Tyr) in the neuraminidase gene.

None of the patients in our study were known to have received amantadine. However, we detected amantadine-resistant viruses among both A/H1N1 (62.0%) and A/H3N2 (100%) viruses at a high frequency during the 2007–2008 influenza season. The high prevalence of amantadine-resistant A/H1N1 strains detected in Japan was one season before the 2006–2007 season, and that of the A/H3N2 strains was the previous two seasons (2005–2006 and 2006–2007) (29, 30, 32). The source of the international spread of amantadine-resistant strains is speculated to be Southeast and East Asia (6). In particular, in China, information from the Nonprescription Medicines Association shows that amantadine is available in over-the-counter formulations and is included in various cold remedies for which humans do not need prescriptions, and chicken farmers frequently add amantadine to chicken food or water for the treatment and prophylaxis of avian influenza virus and other viral diseases with low levels of pathogenicity (15). In addition, amantadine-resistant strains that could be efficiently transmitted without drug pressure were eventually generated by genetic reassortment (18).

TABLE 3. Rate of amantadine resistance among influenza A virus isolates in the 2007–2008 season in Japan[a]

Subtype	No. of isolates: Influenza A virus	No. of isolates: Amantadine-resistant virus[b]	Rate (%) of amantadine-resistant viruses
H1N1	663	411	62.0
H3N2	56	56	100.0

[a] Samples were collected from individuals in the Hokkaido, Gunma, Niigata, Kyoto, Hyogo, and Nagasaki Prefectures in Japan.
[b] Amantadine resistance was conferred by the Ser31Asn mutation in the M2 gene.

Recently, a high rate of resistance to oseltamivir was detected among A/H1N1 viruses in several countries in different regions of the world in 2007 and 2008 (35), and combined treatment with adamantane and neuraminidase inhibitors should be considered for high-risk patients when the subtype is unknown (12). However, monitoring of influenza viruses for resistance to both drugs is crucial when combination treatment is used.

In conclusion, this study shows that the cycling probe method can specifically and rapidly detect amantadine-resistant influenza A viruses with the Ser31Asn mutation in the M2 gene directly from nasopharyngeal swab specimens and is quite useful for monitoring for drug-resistant strains to elicit the judicial use of amantadine for chemoprophylaxis and the treatment of influenza.

ACKNOWLEDGMENTS

This study was supported by a research grant from the Kurozumi Medical Foundation.

We thank Junko Yamamoto, Kazuhide Okazawa, and Kentaro Moro of Takara Bio Inc. for technical assistance in developing the cycling probe assay. We thank clinical doctors Rika Sugai in Hokkaido Prefecture; Takashi Kawashima in Gunma Prefecture;, Isamu Sato in Niigata Prefecture; Shigeyoshi Hibi, Satoshi Ikushima, Fumitomo Fujiwara, and Kentaro Tsunamoto in Kyoto Prefecture; Tetsuo Hashida in Hyogo Prefecture; and Hironori Masaki, Yutaka Shirahige, Hidehumi Ishikawa, Satoshi Degawa, Noritika Asou, and Hironobu Kageura in Nagasaki Prefecture. We are grateful to Akinori Miyashita and Ryozo Kuwano in the Department of Molecular Genetics, Bioresource Science Branch, Center for Bioresources, Brain Research Institute, Niigata University, for utilization of their DNA sequencer. We thank Akemi Watanabe for technical assistance with virus isolation and Yoshiko Kato for intensive secretarial work.

REFERENCES

1. **Barr, I., Y. Deng, P. Iannello, A. Hurt, and N. Komadina.** 2008. Adamantane resistance in influenza A(H1) viruses increased in 2007 in South East Asia but decreased in Australia and some other countries. Antivir. Res. **80:**200–205.
2. **Barr, I., A. Hurt, P. Iannello, C. Tomasov, N. Deed, and N. Komadina.** 2007. Increased adamantane resistance in influenza A(H3) viruses in Australia and neighbouring countries in 2005. Antivir. Res. **73:**112–117.
3. **Bekkaoui, F., I. Poisson, W. Crosby, L. Cloney, and P. Duck.** 1996. Cycling probe technology with RNase H attached to an oligonucleotide. Biotechniques **20:**240–248.
4. **Belshe, R., B. Burk, F. Newman, R. Cerruti, and I. Sim.** 1989. Resistance of influenza A virus to amantadine and rimantadine: results of one decade of surveillance. J. Infect. Dis. **159:**430–435.
5. **Bolotin, S., A. Robertson, A. Eshaghi, C. De Lima, E. Lombos, E. Chong-King, L. Burton, T. Mazzulli, and S. Drews.** 2009. Development of a novel real-time reverse-transcriptase PCR method for the detection of H275Y positive influenza A H1N1 isolates. J. Virol. Methods **158:**190–194.
6. **Bright, R., M. Medina, X. Xu, G. Perez-Oronoz, T. Wallis, X. Davis, L. Povinelli, N. Cox, and A. Klimov.** 2005. Incidence of adamantane resistance among influenza A (H3N2) viruses isolated worldwide from 1994 to 2005: a cause for concern. Lancet **366:**1175–1181.
7. **Bright, R., D. Shay, B. Shu, N. Cox, and A. Klimov.** 2006. Adamantane resistance among influenza A viruses isolated early during the 2005–2006 influenza season in the United States. JAMA **295:**891–894.
8. **Deyde, V., and L. Gubareva.** 2009. Influenza genome analysis using pyrosequencing method: current applications for a moving target. Expert Rev. Mol. Diagn. **9:**493–509.
9. **Deyde, V., X. Xu, R. Bright, M. Shaw, C. Smith, Y. Zhang, Y. Shu, L. Gubareva, N. Cox, and A. Klimov.** 2007. Surveillance of resistance to adamantanes among influenza A(H3N2) and A(H1N1) viruses isolated worldwide. J. Infect. Dis. **196:**249–257.
10. **Duck, P., G. Alvarado-Urbina, B. Burdick, and B. Collier.** 1990. Probe amplifier system based on chimeric cycling oligonucleotides. Biotechniques **9:**142–148.
11. **Duwe, S., and B. Schweiger.** 2008. A new and rapid genotypic assay for the detection of neuraminidase inhibitor resistant influenza A viruses of subtype H1N1, H3N2, and H5N1. J. Virol. Methods **153:**134–141.
12. **Fiore, A., D. Shay, K. Broder, J. Iskander, T. Uyeki, G. Mootrey, J. Bresee, and N. Cox.** 2008. Prevention and control of influenza: recommendations of the Advisory Committee on Immunization Practices (ACIP), 2008. MMWR Recommend. Rep. **57:**1–60.
13. **Hall, C., R. Dolin, C. Gala, D. Markovitz, Y. Zhang, P. Madore, F. Disney, W. Talpey, J. Green, and A. Francis.** 1987. Children with influenza A infection: treatment with rimantadine. Pediatrics **80:**275–282.
14. **Hall, T. A.** 1999. BioEdit: a user-friendly biological sequence alignment editor and analysis program for Windows 95/98/NT. Nucleic Acids Symp. Ser. **41:**95–98.
15. **He, G., J. Qiao, C. Dong, C. He, L. Zhao, and Y. Tian.** 2008. Amantadine-resistance among H5N1 avian influenza viruses isolated in northern China. Antivir. Res. **77:**72–76.
16. **Hoffmann, E., J. Stech, Y. Guan, R. Webster, and D. Perez.** 2001. Universal primer set for the full-length amplification of all influenza A viruses. Arch. Virol. **146:**2275–2289.
17. **Hogrefe, H., R. Hogrefe, R. Walder, and J. Walder.** 1990. Kinetic analysis of Escherichia coli RNase H using DNA-RNA-DNA/DNA substrates. J. Biol. Chem. **265:**5561–5566.
18. **Holmes, E., E. Ghedin, N. Miller, J. Taylor, Y. Bao, K. St. George, B. Grenfell, S. Salzberg, C. Fraser, D. Lipman, and J. Taubenberger.** 2005. Whole-genome analysis of human influenza A virus reveals multiple persistent lineages and reassortment among recent H3N2 viruses. PLoS Biol. **3:**e300.
19. **Holsinger, L., D. Nichani, L. Pinto, and R. Lamb.** 1994. Influenza A virus M2 ion channel protein: a structure-function analysis. J. Virol. **68:**1551–1563.
20. **Joshi, M., H. Keith Pittman, C. Haisch, and K. Verbanac.** 2008. Real-time PCR to determine transgene copy number and to quantitate the biolocalization of adoptively transferred cells from EGFP-transgenic mice. Biotechniques **45:**247–258.
21. **Klimov, A., E. Rocha, F. Hayden, P. Shult, L. Roumillat, and N. Cox.** 1995. Prolonged shedding of amantadine-resistant influenzae A viruses by immunodeficient patients: detection by polymerase chain reaction-restriction analysis. J. Infect. Dis. **172:**1352–1355.
22. **Lee, C., and D. Suarez.** 2004. Application of real-time RT-PCR for the quantitation and competitive replication study of H5 and H7 subtype avian influenza virus. J. Virol. Methods **119:**151–158.
23. **Marshall, R., M. Chernesky, D. Jang, E. Hook, C. Cartwright, B. Howell-Adams, S. Ho, J. Welk, J. Lai-Zhang, J. Brashear, B. Diedrich, K. Otis, E. Webb, J. Robinson, and H. Yu.** 2007. Characteristics of the m2000 automated sample preparation and multiplex real-time PCR system for detection of Chlamydia trachomatis and Neisseria gonorrhoeae. J. Clin. Microbiol. **45:**747–751.
24. **Masuda, H., H. Suzuki, H. Oshitani, R. Saitō, S. Kawasaki, M. Nishikawa, and H. Satoh.** 2000. Incidence of amantadine-resistant influenza A viruses in sentinel surveillance sites and nursing homes in Niigata, Japan. Microbiol. Immunol. **44:**833–839.
25. **Monto, A., and N. Arden.** 1992. Implications of viral resistance to amantadine in control of influenza A. Clin. Infect. Dis. **15:**362–367.
26. **Pinto, L., L. Holsinger, and R. Lamb.** 1992. Influenza virus M2 protein has ion channel activity. Cell **69:**517–528.
27. **Pinto, L., and R. Lamb.** 2007. Controlling influenza virus replication by inhibiting its proton channel. Mol. Biosyst. **3:**18–23.
28. **Reddy, S., and P. Manna.** 2005. Quantitative detection and differentiation of human herpesvirus 6 subtypes in bone marrow transplant patients by using a single real-time polymerase chain reaction assay. Biol. Blood Marrow Transplant. **11:**530–541.
29. **Saito, R., D. Li, and H. Suzuki.** 2007. Amantadine-resistant influenza A (H3N2) virus in Japan, 2005–2006. N. Engl. J. Med. **356:**312–313.
30. **Saito, R., D. Li, Y. Suzuki, I. Sato, H. Masaki, H. Nishimura, T. Kawashima, Y. Shirahige, C. Shimomura, N. Asoh, S. Degawa, H. Ishikawa, M. Sato, Y. Shobugawa, and H. Suzuki.** 2007. High prevalence of amantadine-resistance influenza a (H3N2) in six prefectures, Japan, in the 2005–2006 season. J. Med. Virol. **79:**1569–1576.
31. **Saito, R., H. Oshitani, H. Masuda, and H. Suzuki.** 2002. Detection of amantadine-resistant influenza A virus strains in nursing homes by PCR-restriction fragment length polymorphism analysis with nasopharyngeal swabs. J. Clin. Microbiol. **40:**84–88.
32. **Saito, R., Y. Suzuki, D. Li, H. Zaraket, I. Sato, H. Masaki, T. Kawashima, S. Hibi, Y. Sano, Y. Shobugawa, T. Oguma, and H. Suzuki.** 2008. Increased incidence of adamantane-resistant influenza A(H1N1) and A(H3N2) viruses during the 2006–2007 influenza season in Japan. J. Infect. Dis. **197:**630–632.
33. **Suwannakarn, K., S. Payungporn, T. Chieochansin, R. Samransamruajkit, A. Amonsin, T. Songserm, A. Chaisingh, P. Chamnanpood, S. Chutinimitkul, A. Theamboonlers, and Y. Poovorawan.** 2008. Typing (A/B) and subtyping (H1/H3/H5) of influenza A viruses by multiplex real-time RT-PCR assays. J. Virol. Methods **152:**25–31.
34. **Townsend, M., J. Smagala, E. Dawson, V. Deyde, L. Gubareva, A. Klimov, R. Kuchta, and K. Rowlen.** 2008. Detection of adamantane-resistant influenza on a microarray. J. Clin. Virol. **42:**117–123.
35. **World Health Organization.** 2008, posting date. Influenza A(H1N1) virus resistance to oseltamivir. World Health Organization, Geneva, Switzerland. http://www.who.int/csr/disease/influenza/oseltamivir_summary/en/index.html. Accessed 26 December 2008.

MAJOR ARTICLE

Protective Immunity Afforded by Inactivated H5N1 (NIBRG-14) Vaccine Requires Antibodies against Both Hemagglutinin and Neuraminidase in Mice

Yoshimasa Takahashi,[1] Hideki Hasegawa,[2] Yukari Hara,[1] Manabu Ato,[1] Ai Ninomiya,[3] Hirotaka Takagi,[4] Takato Odagiri,[3] Tetsutaro Sata,[2] Masato Tashiro,[3] and Kazuo Kobayashi[1]

Departments of [1]Immunology, [2]Pathology, and [3]Virology III and [4]Division of Biosafety Control and Research, National Institute of Infectious Diseases, Tokyo, Japan

Background. Hemagglutination-inhibition (HI) antibody titers correlate with protective immunity to seasonal influenza viruses. However, inactivated H5N1 influenza vaccines from Vietnam 2004 strains afford protection without producing high or even detectable HI antibodies.

Methods. BALB/c mice were immunized twice (at a 3-week interval) with inactivated whole-virus influenza vaccine produced using reverse genetics, with the internal genes of A/PR/8/34 (a high-yield strain) and the hemagglutinin (HA) and neuraminidase (NA) genes of A/Vietnam/1194/04 (H5N1) virus (NIBRG-14) adjuvanted with alum (5 μg of HA). Either HA- or NA-binding antibodies were absorbed from the immune serum. The protective efficacy of these antibodies was determined by injecting the absorbed serum into severe combined immunodeficiency mice, which were then challenged with highly pathogenic H5N1 virus (A/Vietnam/Jp1203/2004; Japanese isolate of A/Vietnam/1203/2004).

Results. The NIBRG-14 vaccine elicited levels of anti-HA antibodies similar to levels elicited by the H1N1 vaccines, as well as levels of anti-NA antibodies higher than those elicited by the H1N1 vaccines. The absorption of either anti-HA or anti-NA antibody from immune serum samples obtained from NIBRG-14–vaccinated mice significantly reduced the protective efficacy of the serum.

Conclusions. For NIBRG-14 vaccines to confer protection to vaccinated hosts, both anti-HA and anti-NA antibodies are required. This finding implies that the measurement of both antibody levels may be required for accurate evaluation of vaccine efficacy.

To prepare for the emergence of pandemic viruses, H5N1 vaccine strains have been developed using reverse genetics [1]. However, in several clinical studies, it has been demonstrated that inactivated H5N1 vaccines induce lower levels of hemagglutination-inhibition (HI) and microneutralization (MN) antibody (Ab) titers than do seasonal influenza vaccines [2–6]. H5N1 viruses or vaccines derived from Vietnam 2004 strains poorly induced HI and MN Abs in immunologically naive ferrets and mice; this finding suggests that the immunogenicity of the vaccines, rather than the immunologic status of the vaccinated host, is responsible for the weak Ab response [7, 8]. Moreover, when influenza virus that bears a Ser223→Asn223 substitution in the hemagglutinin (HA) of Vietnam 2004 strains was used as detection antigen, the sensitivity of the HI test improved, demonstrating that the insufficient sensitivity of the HI test is also involved in the process [7].

The HI test predominantly detects anti-HA Abs, which are primarily responsible for virus neutralization in vivo. Therefore, the HI Ab titer is widely used as an immune correlate of vaccine efficacy [9]. However, H5N1 vaccines or viruses confer protection against Vietnam 2004 strains without there being any significant increase in HI titers [7, 8, 10]; this finding implies that the

Received 27 October 2008; accepted 19 December 2008; electronically published 22 April 2009.

Potential conflicts of interest: none reported.

Presented in part: 55th Annual Meeting of the Japanese Society for Virology, Sapporo, Japan, 21–23 October 2007 (abstract 3E09); 37th Annual Meeting of the Japanese Society for Immunology, Tokyo, Japan, 20–22 November 2007 (abstract 1-E-W9-2-P).

Financial support: Regulatory Science Project of the Ministry of Health, Labour and Welfare of Japan, Emerging and Re-emerging Infectious Diseases of the Ministry of Health, Labour and Welfare of Japan, and Ministry of Education, Culture, Sports, Science and Technology of Japan.

Reprints or correspondence: Dr. Yoshimasa Takahashi, 1-23-1 Toyama, Shinjuku, Tokyo, 162-8640 Japan (ytakahas@nih.go.jp).

The Journal of Infectious Diseases 2009; 199:1629–37

0022-1899/2009/19911-0011$15.00
DOI: 10.1086/598954

protective immunity provided by H5N1 vaccines requires immune components that cannot be detected by the HI test. The details of this protection and the immune correlates of vaccine efficacy remain to be determined.

In addition to the HA protein, the NA protein of influenza viruses can be the target of the protective Ab response. Although HA and NA are equivalently immunogenic on a molecular basis [11], the Ab response to NA is significantly suppressed when NA is presented in conjugation with HA. This phenomenon is known as intravirionic antigenic competition [12]. Thus, anti-NA Ab titers generated by whole inactivated vaccines are usually lower than those generated by immunization with equivalent amounts of purified NA, which may lead to less of a contribution of anti-NA Abs to protective immunity elicited by seasonal influenza vaccines.

Using a mouse model, we examined the relative contribution of anti-HA and anti-NA Abs elicited by whole inactivated H5N1 (NIBRG-14) vaccines adjuvanted with alum toward the induction of protective immunity. It was observed that the NIBRG-14 vaccine elicited anti-HA Abs with low HI and MN activity and higher levels of anti-NA Abs than did H1N1 vaccines. Of note, both anti-HA and anti-NA Abs are required for sufficient protection against infection with the highly pathogenic H5N1 virus. The data provide new insights into the protective immunity provided by H5N1 vaccines and prompt further investigation into the immune correlates of vaccine efficacy.

METHODS

Vaccine preparation. NIBRG-14 (H5N1) virus, which possesses modified HA and NA genes derived from the A/Vietnam/1194/2004 strain in the backbone of 6 internal genes of A/Puerto Rico/8/34 (PR8), was provided by the National Institute for Biological Standards and Controls. NIBRG-14, PR8 (H1N1), and A/New Caledonia/20/99 (NC20, H1N1) viruses were propagated in the allantoic cavity of the eggs of a 10-day-old embryonated hen and were purified through a 10%–50% sucrose gradient by means of ultracentrifugation. Viruses were resuspended in phosphate-buffered saline and were inactivated by treatment with 0.05% formalin at 4°C for 2 weeks. The protein and HA concentrations of the whole inactivated vaccines were determined as reported elsewhere [8]. The whole inactivated vaccines and alum solution (Pierce) were mixed in a 3:1 ratio and incubated at room temperature for 1 h before use.

Mice, vaccination, and challenge. BALB/c mice (age, 6–8 weeks; body weight [± standard deviation {SD}], 20.0 ± 0.8 g; Japan SLC) were subcutaneously primed with whole inactivated vaccines that contained 5 μg of HA and were boosted with the same vaccines at a 3-week interval. Two weeks later, serum samples were collected from each mouse. For virus challenge, anesthetized CB17–severe combined immunodeficient (SCID) mice (age, 8 weeks; body weight [±SD], 20.3 ± 0.6 g; CLEA Japan) were challenged intranasally with a lethal dose (5 × 50% lethal dose, 5 LD_{50}) of PR8 or A/VN/Jp1203/04 (volume, 20 μL) and monitored daily for survival. All experiments with highly pathogenic viruses were conducted in a biosafety level 3 containment facility. All mice were treated in accordance with the guidelines of the institutional animal care and use committee of the National Institute of Infectious Diseases (Tokyo, Japan).

Baculoviral expression of recombinant HA (rHA) and recombinant NA (rNA). The HA and NA coding genes of NIBRG-14, PR8, and NC20 strains were amplified by polymerase chain reaction (PCR) to attach a 6× His tag to the C-terminal of HA and the N-terminal of NA. The amplified DNAs were cloned into pBacPAK8 (Clontech) and transfected into Sf-21 *(Spodoptera frugiperda)* insect cells. Recombinant baculoviruses that contained rHA and rNA genes were isolated, and Sf-21 cells were infected with them. The recombinant proteins tagged with 6× His were purified using Talon columns (Clontech), in accordance with the manufacturer's protocol. The purity of the purified proteins was analyzed using 10% sodium dodecyl sulfate–polyacrylamide gel electrophoresis.

Detection of serum Abs. Serum Abs against vaccine viruses were detected using an HI test performed with red blood cells from chickens, MN assay, and enzyme-linked immunosorbent assay (ELISA). The HI and MN assays were performed as described elsewhere [8], and titers below the limit of detection were assigned a value that was one-half of that limit. The concentrations of HA- or NA-binding immunoglobulin G1 (IgG1) Abs were determined by ELISA performed using baculovirus-produced rHA and rNA proteins as the coating antigen. Ninety-six–well plates were coated with 10 μg/mL rHA or rNA in 0.1 mol/L carbonate buffer (pH 9.0) at 4°C and blocked with 1% bovine serum albumin. For the use of rNA, 0.3 mmol/L Ca^{2+} was included in carbonate buffer to increase stability. Serially diluted serum samples were then added to each well, along with standard serum samples obtained from hyperimmunized mice. Horseradish peroxidase–conjugated goat anti–mouse immunoglobulin G1 (Southern Biotechnology) was added, and horseradish peroxidase activity was visualized using o-phenylenediamine dihydrochloride (Sigma). The relative concentrations of anti-HA or anti-NA antibodies were estimated by comparison to standard curves on each plate.

Detection of virus attachment by flow cytometry. The inactivated viruses were labeled with AlexaFluor647 (Invitrogen), and HA activity was determined using red blood cells from chickens. We confirmed that the HA activities of the inactivated viruses were not affected by the labeling procedure. After preincubation of the AlexaFluor647-labeled inactivated viruses (equivalent to 4HA) with 1/100-diluted heat-inactivated immune serum, the mixtures were added to Madin-Darby canine kidney (MDCK) cells (1×10^5 cells) and were further incubated at 4°C for 30 min. The stained cells were analyzed using FACS Vantage (BD Immunocytometry Systems), and the mean fluorescence intensity was analyzed using FlowJo software, version 8.8.2 (TreeStar).

Absorption of HA- and NA-binding serum Abs. His-tagged rHA and rNA proteins (1 mg) were conjugated with 1 mg of

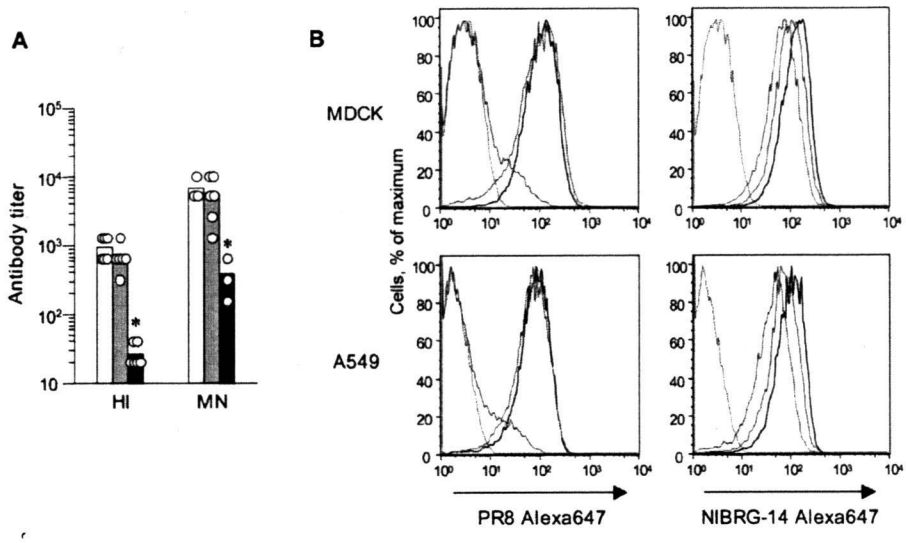

Figure 1. Poor inhibition of virus attachment in vitro by serum antibodies (Abs) elicited by the NIBRG-14 vaccine. *A,* Serum samples collected from PR8-, NC20-, or NIBRG-14–vaccinated mice (denoted by *white, gray,* and *black,* respectively) and determination of hemagglutination-inhibition (HI) and microneutralization (MN) activities of serum samples by use of homologous viruses. $*P < .05$, by Mann-Whitney nonparametric test (for HI) and Student's *t* test (for MN). *B,* Analysis of amounts of inactivated PR8 or NIBRG-14 viruses attached to Madin-Darby canine kidney (MDCK) or A549 cells *(black lines).* Inactivated viruses were preincubated with anti-PR8 serum *(blue lines)* or anti–NIBRG-14 serum *(red lines)* to estimate the inhibitory effects of each serum type. The data are representative of 3 independent experiments.

Talon resin (Clontech), and 3 mL of serum was applied onto the column that contained the rHA- or rNA-conjugated Talon resin. The flow-through was collected and applied again to repeat the absorption procedure twice. To estimate the protective efficacy of the serum Abs, 200 μL of serum that was deficient in HA- or NA-binding Abs was intravenously administered into the tail vein of CB17-SCID mice. The mice were challenged with 5 LD_{50} of PR8 or A/VN/Jp1203/04 (volume, 20 μL) viruses 6 h later.

Histopathologic examination and immunohistochemical (IHC) analysis. Mice were killed and dissected ventrally along the median line from the xiphoid process to the point of the chin. Excised lung, brain, and nasal tissue specimens were fixed with

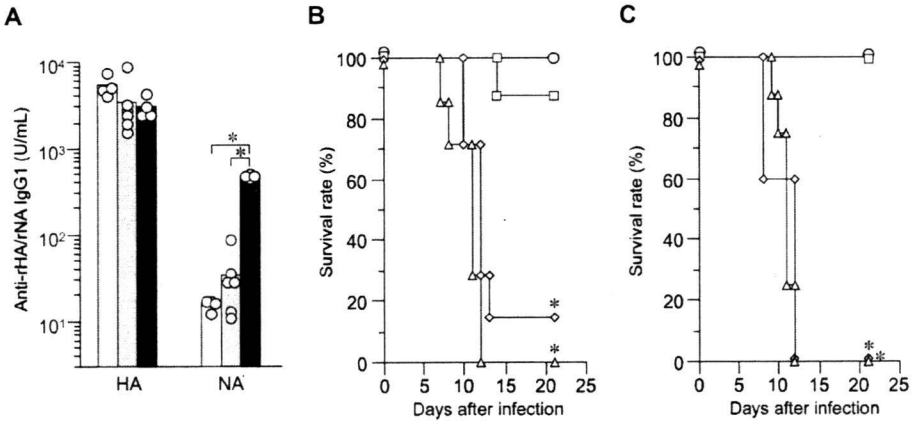

Figure 2. Levels of anti–hemagglutinin (HA)/neuraminidase (NA) serum antibodies (Abs) and the protection provided by immune serum. *A,* Anti–recombinant HA (rHA)/recombinant NA (rNA) immunoglobulin G1 (IgG1) Ab titers in the serum of PR8-, NC20-, or NIBRG-14–vaccinated mice (denoted by *white, gray,* and *black bars,* respectively) were determined by enzyme-linked immunosorbent assay. Each circle denotes the result obtained for an individual mouse. $*P < .05$, by Mann-Whitney nonparametric test (2-tailed test). *B* and *C,* CB17–severe combined immunodeficient (SCID) mice were administered 200 μL of serially diluted serum (*circles,* 1:1; *squares,* 1:2; *diamonds,* 1:4; and *triangles,* 1:20) obtained from mice vaccinated with NIBRG-14 *(B)* or PR8 *(C).* The mice were challenged with a lethal dose of A/VN/Jp1203/04 *(B)* or PR8 *(C),* and then survival curves were created using the Kaplan-Meier method. The generalized Wilcoxon test was used to calculate *P* values for the mice that were administered nondiluted and diluted serum. The data are representative of 2 independent experiments.

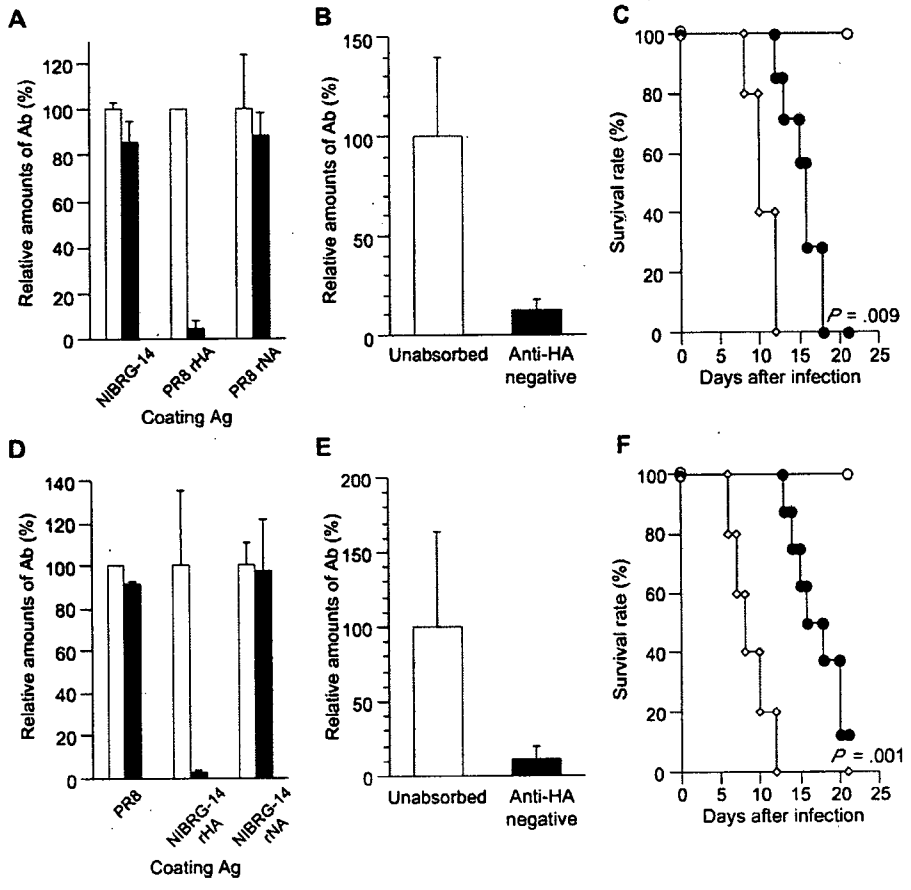

Figure 3. Protective role of hemagglutinin (HA)–binding antibodies (Abs) against homologous virus challenge. Immune serum samples obtained from mice that were vaccinated with PR8 *(A–C)* or NIBRG-14 *(D–F)* were applied to recombinant HA (rHA)–conjugated columns, and HA-binding Abs were absorbed. *A* and *D*, Amounts of immunoglobulin G1 Abs to rHA, recombinant neuraminidase (rNA), NIBRG-14 virus *(A)*, and PR8 virus *(D)* were determined by enzyme-linked immunosorbent assay and are expressed as the relative amounts against those of unabsorbed serum. *White bars* and *black bars* denote unabsorbed control and absorbed serum samples, respectively. Data are the mean ± standard deviation (SD) ($n = 3$). *B* and *E*, Amounts of neutralizing Abs were estimated by microneutralization (MN) assays performed using PR8 *(B)* and NIBRG-14 *(E)* as challenge viruses. Ab titers are expressed as relative amounts, compared with Ab titers of unabsorbed serum. Data are the mean ± SD ($n = 3$). *C* and *F*, CB17–severe combined immunodeficient (SCID) mice were administered 200 μL of serum, which had been passed through rHA-conjugated columns *(black circles)* or columns not conjugated with rHA HA *(white circles)*. As unprotected controls, serum samples from mice that were primed only with alum were also injected *(white diamonds)*. The mice were challenged with a lethal dose of PR8 *(C)* or A/VN/Jp1203/04 *(F)*. Survival curves were then created. The generalized Wilcoxon test was used to calculate *P* values for the mice that were administered absorbed serum or unabsorbed control serum. The data are representative of 2 independent experiments. Ag, antigen.

10% neutral-buffered formalin. The nasal tissue specimens were decalcified in ethylenediaminetetraacetic acid solution. After fixation, tissues were embedded in paraffin by use of conventional methods and were stained with hematoxylin-eosin or subjected to IHC staining using antiserum against the nucleoprotein of PR8 virus. IHC staining was performed using 3-3' diaminobenzidine as the substrate.

RESULTS

Poor inhibition of the virus attachment by serum Abs induced by NIBRG-14 vaccine. Serum Ab titers of vaccinated mice were evaluated by performing HI and MN assays. Consistent with reports published elsewhere [7, 8, 10], the levels of both HI and MN Abs were lower in mice vaccinated with NIBRG-14 than in mice vaccinated with PR8 and NC20 (figure 1*A*). HI and MN assays measure the level of anti-HA Abs, which block virus attachment to sialylated cellular receptors. In addition, the MN assay used in the present study detects anti-NA Abs at a lower sensitivity [13]. To confirm that the immune serum elicited by NIBRG-14 poorly inhibits virus attachment to cellular receptors, we quantitated the viruses attached to MDCK cells by means of flow cytometry. It was observed that both inactivated viruses exhibited similar levels of attachment to MDCK cells (figure 1*B*). Pretreatment of PR8 virus with anti-PR8 serum

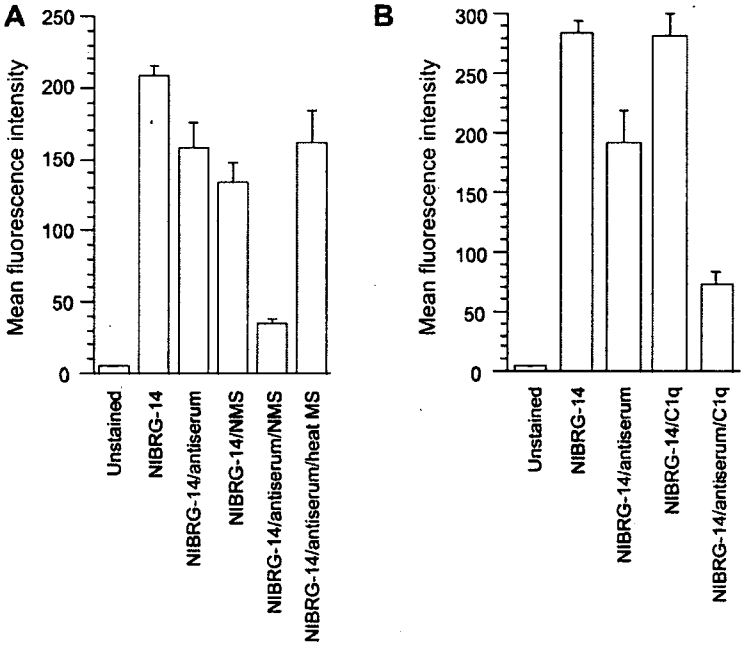

Figure 4. Complement enhanced the inhibition of virus attachment by immune serum. The mean fluorescence intensity of the viruses attached to Madin-Darby canine kidney (MDCK) cells was determined by flow cytometry, as shown in figure 2*B*. *A*, Inactivated NIBRG-14 viruses were preincubated with anti–NIBRG-14 serum in the presence or absence of naive mouse serum (NMS) or heat-inactivated naive mouse serum (heat MS) (final 10%). *B*, Inactivated NIBRG-14 viruses were preincubated in the presence or absence of purified human C1q (10 μg/mL). Data are the mean ± standard deviation (n = 3). Data are representative of 2 independent experiments.

completely inhibited virus attachment, whereas pretreatment of NIBRG-14 virus with anti-NIBRG-14 serum did not inhibit the attachment of NIBRG-14 virus. A similar result was obtained using type II alveolar epithelial cell line A549, which showed that anti–NIBRG-14 serum cannot efficiently inhibit virus attachment, irrespective of the cell type used.

Efficient elicitation of protective serum Abs by NIBRG-14 vaccine in vivo. The poor HI and MN activity of serum from NIBRG-14–vaccinated mice could be attributed to the small quantity or compromised activity of HA-binding Abs. To examine this possibility, the levels of serum Abs specific to HA and NA were determined by ELISA performed using rHA and rNA as antigens. When alum was used as an adjuvant, it was observed that the IgG1 isotype dominated the specific Ab response [14]; therefore, we examined the levels of HA- and NA-binding IgG1 titers in the serum of vaccinated mice (figure 2*A*). Inactivated NIBRG-14, PR8, and NC20 vaccines elicited similar amounts of HA-binding IgG1 Abs, suggesting that the H5 protein of NIBRG-14 possesses sufficient immunogenicity in this immunization protocol. In contrast, NIBRG-14 vaccines induced significantly higher levels of NA-binding IgG1 Ab than did PR8 and NC20 vaccines. This increase in Ab levels was not the result of a lack of sensitivity in the detection of Abs specific for PR8 and NC20 rNAs, because PR8 rNA captured anti-NA Abs induced by NIBRG-14 vaccine at levels >14-fold higher than those induced by H1N1 vaccines. These results suggest that the N1 protein of NIBRG-14 might be more immunogenic and/or stable than those of PR8 and NC20, which easily undergo degradation without Ca^{2+} [15].

The protective immunity induced by subcutaneous injection of alum-adjuvanted inactivated influenza vaccines largely depends on the generation of neutralizing Abs in the serum samples, and the transfer of 200 μL of anti–NIBRG-14 serum from vaccinated mice into immunocompromised SCID mice conferred protection against lethal challenge with H5N1 virus (figure 2*B*). Serial dilution of anti–NIBRG-14 serum and anti-PR8 serum comparably reduced their protective efficacy, and the 4-fold dilution of both types of serum diminished their protective effect. These results suggest that inactivated NIBRG-14 vaccines have sufficient immunogenicity and induce the generation of protective virus-binding Abs, compared with inactivated H1N1 vaccines, although their HI and MN activities are low.

Contribution of non–HI, HA-binding Abs to protection. The protective role of anti-HA Abs in vivo was investigated. After the absorption of HA-binding Abs, levels of residual HA-binding Abs were determined by ELISA and expressed as the percentage of unabsorbed controls. Results showed that the amount of HA-binding Abs in the postabsorbed serum from both NIBRG-14–vaccinated and PR8-vaccinated mice was reduced to <5% of the amount in the unabsorbed control serum (figure 3*A* and 3*D*). MN Ab titers in the absorbed serum from both NIBRG-14–vaccinated and PR8-vaccinated mice were also reduced to approximately one-